Environmental and Endogenous Peroxisome Proliferator-Activated Receptor γ Agonists Induce Bone Marrow B Cell Growth Arrest and Apoptosis: Interactions between Mono(2-ethylhexyl)phthalate, 9-*cis*-Retinoic Acid, and 15-Deoxy-$\Delta^{12,14}$-prostaglandin J_2[1]

Jennifer J. Schlezinger,[2]* Gregory J. Howard,* Christopher H. Hurst,† Jessica K. Emberley,* David J. Waxman,† Thomas Webster,* and David H. Sherr*

The common commercial use of phthalate esters has resulted in significant human exposure to these bioactive compounds. The facts that phthalate ester metabolites, like endogenous PGs, are peroxisome proliferator-activated receptor (PPAR) agonists, and that PPARγ agonists induce lymphocyte apoptosis suggest that phthalate esters are immunosuppressants that could act together with PGs to modulate early B cell development. In this study we examined the effects of a metabolite of one environmental phthalate, mono(2-ethylhexyl)phthalate (MEHP), and 15-deoxy-$\Delta^{12,14}$-PGJ_2 (15d-PGJ_2), on developing B cells. MEHP inhibited [^{3}H]thymidine incorporation by primary murine bone marrow B cells and a nontransformed murine pro/pre-B cell line (BU-11). Cotreatment with a retinoid X receptor α ligand, 9-*cis*-retinoic acid, decreased [^{3}H]thymidine incorporation synergistically, thereby implicating activation of a PPARγ-retinoid X receptor α complex. These results were similar to those obtained with the natural PPARγ ligand 15d-PGJ_2. At moderate MEHP concentrations (25 or 100 μM for primary pro-B cells and a pro/pre-B cell line, respectively), inhibition of [^{3}H]thymidine incorporation resulted primarily from apoptosis induction, whereas at lower concentrations, the inhibition probably reflected growth arrest without apoptosis. Cotreatment of bone marrow B cells with 15d-PGJ_2 and MEHP significantly enhanced the inhibition of [^{3}H]thymidine incorporation seen with MEHP alone, potentially mimicking exposure in the bone marrow microenvironment where PG concentrations are high. Finally, MEHP- and 15d-PGJ_2-induced death does not result from a decrease in NF-κB activation. These data demonstrate that environmental phthalates can cooperate with an endogenous ligand, 15d-PGJ_2, to inhibit proliferation of and induce apoptosis in developing bone marrow B cells, potentially via PPARγ activation. ***The Journal of Immunology,*** **2004, 173: 3165–3177.**

Phthalate esters are ubiquitous environmental contaminants that are produced for a variety of common industrial and commercial purposes. Worldwide, >18 billion pounds of phthalates are produced yearly, mainly for use as plasticizers in polyvinyl chloride products, such as car seats, toys, and bloodbags (1, 2). The annual global production of di(2-ethylhexyl)phthalate (DEHP),[3] the main plasticizer used in the production of polyvinyl chloride, is 3–4 million tons (1). The average daily human exposure to DEHP and its metabolite, mono(2-ethylhexyl)phthalate (MEHP), has been estimated to be 0.6–0.7 μg/kg/day and may be as high 30–40 μg/kg/day in occupationally exposed populations (2–5). Exposure to DEHP from a blood transfusion alone can be as high as 3–4 mg/kg for an adult weighing 70 kg (6), and concentrations of DEHP in blood can range from 50–350 μM (7). DEHP exposure alone has been linked to hepatocarcinogenesis (8) and ovarian (9), testicular (10, 11), and developmental (12) toxicity.

Recently, MEHP as well as many other phthalate esters were shown to be agonists for peroxisome proliferator-activated receptors (PPARs) (13–16). PPARs are members of a nuclear hormone receptor superfamily and are comprised of three subtypes, α, δ, and γ. After ligand binding, the PPAR forms a heterodimeric complex with the retinoid X receptor α (RXRα), initiating a conformational change that results in the dissociation of corepressors, the association of coactivators, and receptor complex binding to PPAR-response elements (5′-AACTAGGNCA A AGGTCA-3′; the consensus sequences are underlined) in genes such as acyl-CoA oxidase and cytochrome P450 4A (17). Transcriptional activity may be enhanced in the presence of ligands for both PPAR and RXRα (18–21). It has been assumed, but not proven, that this enhancement is synergistic rather than additive.

PPARα is expressed highly in metabolically active tissues, such as liver, heart, and kidney (22), and recently has been found to be expressed in myeloid and lymphoid cells (23). PPARα regulates the uptake, activation, and β-oxidation of fatty acids (22). Its agonists induce peroxisome proliferation, hepatomegaly, and hepatocellular

*Department of Environmental Health, Boston University School of Public Health, Boston, MA 02118; and †Department of Biology, Division of Cell and Molecular Biology, Boston University, Boston, MA 02215

Received for publication September 29, 2003. Accepted for publication June 25, 2004.

The costs of publication of this article were defrayed in part by the payment of page charges. This article must therefore be hereby marked *advertisement* in accordance with 18 U.S.C. Section 1734 solely to indicate this fact.

[1] This work was supported by National Institutes of Health Grants RO1ES06086 and PO1HL68705, and Superfund Basic Research Grant 1P42ES 07381. C.H.H. was supported in part by National Research Scientist Award F32ES11105 from the National Institutes of Health.

[2] Address correspondence and reprint requests to Dr. Jennifer J. Schlezinger, Boston University School of Public Health, Department of Environmental Health, 715 Albany Street, R-405 Boston, MA 02118. E-mail address: jschlezi@bu.edu

[3] Abbreviations used in this paper: DEHP, di(2-ethylhexy)phthalate; 9-*cis*-RA, 9-*cis*-retinoic acid; Luc, luciferase; MEHP, mono(2-ethylhexyl)phthalate; PI, propidium iodide; PLSD, protected least significant difference; PPAR, peroxisome proliferator-activated receptor; PPRE, peroxisome proliferator response element; 15d-PGJ_2, 15-deoxy-$\Delta^{12,14}$-PGJ_2; 9-*cis*-RA, 9-*cis*-retinoic acid; RXR, retinoid X receptor.

0022-1767/04/$02.00

carcinoma (as reviewed in Ref. 24) as well as splenic and thymic atrophy (25) in rodents in a PPARα-dependent manner. MEHP, the active metabolite of DEHP, transcriptionally activates PPARα (15, 16). However, PPARα activation alone cannot explain the renal, testicular, or reproductive toxicity or teratogenicity of DEHP, because PPARα-null and wild-type mice are equally susceptible to these DEHP-induced toxic effects (8, 11, 26, 27).

PPARγ1 is expressed highly in the immune system (28, 29), particularly in mouse and human tissues that contain high percentages of B cells, such as spleen, lymph nodes, and bone marrow (23, 28, 30–32). PPARγ plays an important role not only in regulating adipocyte differentiation (33) and insulin responsiveness (34), but also in immune function, particularly in macrophage inflammatory responses (35–37), T cell activation (38, 39), and dendritic cell maturation (40). Notably, a reduction of PPARγ expression in haploinsufficient mice increases B cell proliferative responses (41), suggesting an important role for this receptor in B cell growth regulation. MEHP transcriptionally activates PPARγ (15, 16) and stimulates adipogenesis, a PPARγ-dependent process (14), suggesting a molecular mechanism through which environmental phthalates may compromise B cell function.

PPARγ agonists, including 15-deoxy-$\Delta^{12,14}$-PGJ_2 (15d-PGJ_2) and glitazone drugs, induce apoptosis in monocytes (37), T cells (42), and B cells (30, 31). Treatment of murine primary bone marrow B cells, a nontransformed murine pro/pre-B cell line, or a transformed murine immature B cell line with drugs that target PPARγ (ciglitazone and GW347845X) induces PPARγ-peroxisome proliferator response element (PPRE) binding, NF-κB upregulation, and rapid apoptosis (31). Cotreatment with 9-*cis*-retinoic acid (9-*cis*-RA) decreases the PPARγ agonist dose required to activate NF-κB and induce apoptosis. These data suggest that activation of PPARγ-RXR initiates a potent apoptotic signaling cascade in B cells through PPARγ activation and possibly NF-κB regulation. However, they do not reveal how environmental PPARγ ligands may affect developing lymphocytes, nor do they address the consequences of coactivation of PPARγ with environmental and endogenous agonists such as MEHP and 15d-PGJ_2, respectively.

The facts that common environmental phthalate ester metabolites are PPAR agonists and that PPARγ agonists induce lymphocyte apoptosis suggest that environmental phthalate esters may be important immunosuppressants. Furthermore, the effect of PPARγ haploinsufficiency on B cell proliferation suggests PPARγ agonist regulation of B cell growth as well as death. Finally, the high bone marrow concentrations of PGD_2, the precursor to the potent PPARγ agonist, 15d-PGJ_2 (43–45), may lower the threshold of B cell responses to environmental PPARγ agonists. Therefore, we determined whether MEHP, a metabolite of the ubiquitous phthalate DEHP, adversely affects the developing immune system by inducing bone marrow B cell apoptosis and/or growth arrest and whether 15d-PGJ_2 exacerbates these putative effects. The data presented show that MEHP inhibits B cell proliferation and induces apoptosis at relatively low doses, potentially via a signaling cascade involving PPARγ, and that the developing lymphoid system, like many developing organ systems, is particularly susceptible to a spectrum of environmental chemicals, including phthalates.

Materials and Methods

Reagents

9-*Cis*-RA was obtained from Biomol (Plymouth Meeting, PA). The PPARγ-specific Ab was purchased from Calbiochem (San Diego, CA). 15d-PGJ_2 was obtained from Cayman Chemical (Ann Arbor, MI). Plasmocin was purchased from InvivoGen (San Diego, CA). Murine rIL-7 was obtained from Research Diagnostics (Flanders, NJ). The NF-κB and $p27^{kip1}$-specific Abs were purchased from Santa Cruz Biotechnology (Santa Cruz, CA). Troglitazone was obtained from the Sankyo (Tokyo, Japan). Propidium iodide and Protease Inhibitor Cocktail for Mammalian Cells were obtained from Sigma-Aldrich (St. Louis, MO). MEHP was purchased from TCI America (Portland, OR). All other reagents were obtained from Fisher Scientific (Suanee, GA).

Plasmids

The mouse PPARγ expression plasmid pSV-Sport1-PPARγ1 (46) was provided by J. K. Reddy (Northwestern University Medical School, Chicago, IL). The firefly luciferase (Luc) reporter plasmid pHDx3-luc contains three copies of a PPRE derived from the rat enoyl CoA hydratase/3-hydroxyacyl CoA promoter (nt -2956 to -2919) cloned into carbamoyl-phosphate synthetase-Luc reporter (47) and was obtained from Dr. J. Capone (McMaster University, Ontario, Canada). The reporter plasmid pLuc-4A6–880, containing 880 nt of the 5′-flanking DNA of the rabbit CYP4A6 gene cloned into p19Luc was provided by Dr. E. Johnson (The Scripps Research Institute, La Jolla, CA). The *Renilla* luciferase reporter plasmid pRL-CMV was purchased from Promega (Madison, WI).

Bone marrow B cell isolation

B cells were isolated from the bone marrow of 4- to 6-wk-old C57BL/6 male mice and cultured in RPMI 1640 containing 10% FBS, L-glutamine, penicillin/streptomycin, 2-ME, and 16 ng/ml murine rIL-7 for 5–7 days by the method of Tze et al. (48). Before experimentation, these cells (>80% $B220^+/CD43^+$) were purified further using anti-B220 microbeads and a magnetic column (MACS; Miltenyi Biotec, Auburn, CA). After purification, 95.1 $\pm$ 0.5% of the cells were $B220^+/CD43^+$.

Cell lines

The stromal cell-dependent, C57BL/6-derived BU-11 cell line has been characterized previously (49). BU-11 cells represent B cells at the transition between the pro- and early pre-B cell stages as they are $CD43^+/B220^+/IgM^-$ with rearranged Ig H chain genes (50). BMS2 is a culture dish-adherent, cloned bone marrow stromal cell line that supports BU-11 cell growth (51). Stocks of BU-11 cells were maintained on BMS2 cell monolayers in an equal mixture of DMEM and RPMI 1640 medium with 5% FBS, plasmocin, L-glutamine, and 2-ME. For experiments, BU-11 cells were plated without BMS2 in the presence of murine rIL-7 (16 ng/ml). All cultures were maintained at 37°C in a humidified, 7.5% CO_2 atmosphere. COS-1 cells (American Type Culture Collection, Manassas, VA) were grown in DMEM containing 10% FBS (Sigma-Aldrich) and 50 U/ml penicillin/streptomycin (Invitrogen Life Technologies, Carlsbad, CA). Cell cultures were determined to be mycoplasma negative by PCR (*Mycoplasma* Detection Kit; American Type Culture Collection).

[^{3}H]Thymidine incorporation

Primary bone marrow B cells or BU-11 cells were cultured in 96-well plates in medium containing 5% FBS and treated with ethanol (vehicle; final concentration, 0.5%), MEHP (10–200 μM), 15d-PGJ_2 (0.5–20 μM), and/or 9-*cis*-RA (10 μM) for 24 h. ^{3}H-labeled thymidine (1 μCi/well) was added, and the incubation was continued for 24 h. Cells were harvested using a cell harvester (PHD, Cambridge, MA). The [^{3}H]thymidine retained on the filter was detected using a scintillation counter (Beckman Coulter, Fullerton, CA).

Analysis of apoptosis

For propidium iodide (PI) staining, primary bone marrow B cells or BU-11 cells were cultured in 24-well plates in medium containing 5% FBS and were treated with ethanol (vehicle; final concentration, 0.1%), MEHP (50–200 μM), 15d-PGJ_2 (0.5–10 μM), and/or 9-*cis*-RA (10–20 μM) for 8–24 h. Cells were harvested by gentle pipetting; washed once with cold PBS containing 5% FBS and 10 μM azide; resuspended in 0.25 ml of hypotonic buffer containing 50 μg/ml PI, 1% sodium citrate, and 0.1% Triton X-100; and analyzed on a FACScan flow cytometer (BD Biosciences, Mountain View, CA). For apoptosis studies, cells were monitored with Fl-2 output in the log mode. The percentage of cells undergoing apoptosis was determined to be those with a weaker PI fluorescence than cells in the G_0/G_1 phase of the cell cycle (49).

For determination of DNA fragmentation, BU-11 cells were cultured in T25 flasks in medium containing 5% FBS and treated with ethanol (vehicle; final concentration, 0.1%), MEHP (50–200 μM), 15d-PGJ_2 (2–10 μM), and/or 9-*cis*-RA (10–20 μM) for 24 h. DNA was isolated and processed as previously described (31). Before loading on a 1.5% agarose gel, the DNA was quantified and treated with 10 μg/ml RNase A at 37°C for 10 min. DNA was visualized using ethidium bromide staining.

Analysis of cell cycle arrest

Cells were treated as described above for 48 h and stained with PI. Stained cells were analyzed by flow cytometry with Fl-2 output in the linear mode.

The expression of $p27^{Kip1}$ was determined by Western blotting. BU-11 cells were cultured in T75 flasks in medium containing 5% FBS and treated with ethanol (vehicle; final concentration, 0.1%), MEHP (50–100 μM), 15d-PGJ_2 (0.5–2 μM), and/or 9-*cis*-RA (10 μM) for 48 h. Whole cell lysates were prepared as described previously (52). Protein concentrations were determined by the Bradford method. Proteins (30 μg) were resolved on 12% gels, transferred to a 0.2-μm nitrocellulose membrane, and incubated with polyclonal $p27^{Kip1}$-specific Ab (SC-776). The secondary Ab was HRP-linked goat anti-rabbit IgG (Bio-Rad, Hercules, CA). Immunoreactive bands were visualized with ECL and analyzed on a densitometer (Molecular Dynamics, Sunnyvale, CA). To control for equal protein loading, blots were reprobed with a β-actin-specific Ab (Sigma-Aldrich) and analyzed as described above. An untreated BU-11 cell control was run with each Western blot, and the data from experimental samples were normalized by dividing by the density measured in the untreated control.

Analysis of chemical interactions; additive vs synergistic effects

BU-11 cells were cultured in 96-well plates in medium containing 5% FBS; treated with ethanol (vehicle; final concentration, 0.5%), MEHP (25–100 μM), 15d-PGJ_2 (0.5–2.5 μM), and/or 9-*cis*-RA (1–10 μM) for 48 h; and assessed for [^{3}H]thymidine incorporation as described above. The method of isoboles was used to analyze combinations of MEHP with 9-*cis*-RA or 15d-PGJ_2 for synergistic effects (53, 54). The dose of x_a is plotted on one horizontal axis, x_b on the other horizontal axis, and the response on the vertical (z) axis. The dose-response curve for each individual compound lies on the axes. The contours of this surface are called isoboles and denote curves of equal response. The shape of the isoboles provides qualitative information about interactions. Isoboles that are approximately linear with a negative slope suggest an additive effect, using the definition of concentration or Loewe additivity (53, 54). Isoboles that bow toward the origin indicate a greater response than that suggested by additivity, i.e., synergy. The contour plots were created in the R statistical environment (version 1.7.1 for Windows XP; R Foundation, Vienna, Austria; www.r-project.org).

Transient transfections

COS-1 cells were cultured in a 48-well plate and transfected 24 h later using FuGene 6 transfection reagent (Roche, Mannheim, Germany) as previously described (16). The transfection mixture contained 90 ng of luciferase reporter plasmid, 5 ng of PPARγ expression plasmid, and 1 ng of pRL-CMV per well in a volume of 15 μl of DMEM containing 0.3 μl of FuGene 6. Salmon sperm DNA (Stratagene, La Jolla, CA) was added as carrier DNA to give a total of 250 ng of DNA/well. Culture medium was replaced 16–18 h later with serum-free DMEM containing vehicle (DMSO; final concentration, 0.5%), MEHP (20 μM), 15d-PGJ_2 (1–15 μM), or troglitazone (3 μM). After treatment for 24 h, cells were lysed by incubation at 4°C in 200 μl of passive lysis buffer (Promega) for 20 min. Firefly and *Renilla* luciferase activities were measured in cell lysates using a dual reporter assay system (Promega) and a Monolight 2010 luminometer (Analytical Luminescence Laboratory, San Diego, CA). Luciferase activity values were normalized for transfection efficiency using *Renilla* luciferase activity assayed in the same cell lysates (firefly luciferase/*Renilla* luciferase).

EMSA

BU-11 cells were cultured in T75 flasks in medium containing 5% FBS and treated with vehicle (ethanol or DMSO; final concentration, 0.1%), MEHP (100–200 μM), or 15d-PGJ_2 (2.5–5 μM) for 2–24 h. Cells were collected and washed in PBS. Nuclear proteins were extracted as described previously (31).

For determination of PPARγ-DNA binding, a double-stranded oligonucleotide containing the PPRE from the acyl-CoA oxidase gene (5′-GTCGACAGGGGACCAGGACAAAGGTCACGTTCGGGAGTCGAC-3′; the consensus sequences are underlined) was used (44). PPARγ binds to this site with significantly greater affinity than PPARα (55). The DNA probe was end-labeled using T4 polynucleotide kinase (Promega) and [γ-^{32}P]ATP and was purified using a Centrispin-20 column (Princeton Separations, Adelphia, NJ). EMSAs were performed as follows. The ^{32}P-labeled DNA (~0.5 ng, 100,000 cpm) and 4 μg of nuclear protein were combined with buffer (final concentrations: 20 mM HEPES (pH 8), 0.2 mM EDTA, 60 mM sodium chloride, 0.1% Nonidet P-40, 1 mM DTT, and 10% glycerol) and poly(dI-dC) (1 μg) in a final volume of 20 μl. The mixture was incubated at room temperature for 30 min. Polyacrylamide gels (16 cm, 5%) were prerun at 200 V for 30 min. Mixtures were electrophoresed at 200 V for 1.5 h in 0.5× TBE (final concentrations: 44 mM Tris-base (pH 8), 44 mM boric acid, and 0.8 mM EDTA). The gels were dried and exposed to film. The specificity of the shifted bands was determined by including an Ab specific for PPARγ (Calbiochem, La Jolla, CA; 516555) or by including 100× cold oligonucleotides containing the PPRE from the acyl-CoA oxidase gene (see above) or an unrelated site (5′-GAGCCGCAAGTGACTCAGCGCGGATCAATTA-3′).

For determination of NF-κB activation, a double-stranded oligonucleotide containing the NF-κB binding site from the upstream regulatory element of c-*myc* (5′-GATCCAAGTCCGGGTTTTCCCCAACC-3′; the consensus sequence is underlined) was used (56). The DNA probe was end-labeled and purified as described above. EMSAs were performed as follows. The ^{32}P-labeled DNA (~0.5 ng, 50,000 cpm) and 2 μg of nuclear protein were combined with buffer (final concentrations: 10 mM Tris-HCl (pH 7.5), 1 mM EDTA, 100 mM sodium chloride, 0.5 mM magnesium chloride, 1 mM DTT, 20 μg BSA, 10% glycerol, and 0.5% Triton X-100) and poly dI-dC (1 μg) in a final volume of 20 μl. The mixture was incubated at room temperature for 30 min. The gel was run as described above, dried, and exposed to film. For quantification, the gels were analyzed on a PhosphorImager (Molecular Dynamics). The identity of the NF-κB subunits was determined by including Abs specific for p50 (sc-114), p52 (sc-848), Rel A (sc-372), or c-Rel (sc-71).

Statistics

Statistical analyses were performed with StatView (SAS Institute, Cary, NC). Data from a minimum of three experiments are presented as the mean ± SE. Student's t test and one-factor ANOVAs were used to analyze the data. For the ANOVAs, Dunnett's or Fisher's protected least significant difference (PLSD) multiple comparisons tests was used to determine significant differences.

Results

MEHP reduces [^{3}H]thymidine incorporation and induces apoptosis in primary bone marrow B lymphocytes

Previous studies demonstrated that B cells in early stages of development undergo apoptosis when exposed to synthetic PPARγ agonist drugs (30). Given this observation, the presence of a natural PPARγ agonist in the bone marrow (i.e., 15d-PGJ_2), the ability of environmental phthalates to activate PPARγ (13–16), and the relatively high human exposure to environmental phthalate esters, we investigated the potential for environmental phthalate esters to affect developing B lymphocytes. Models of early bone marrow B cell development were chosen because of the increased sensitivity of developing organs in general to environmental chemicals (49, 57, 58).

Primary bone marrow B cells were exposed to increasing concentrations of MEHP. [^{3}H]thymidine incorporation, a measure of cell proliferation and/or survival, was assessed 48 h later. In primary bone marrow $B220^+/CD43^+$ B cells, MEHP caused a significant reduction in [^{3}H]thymidine incorporation at concentrations as low as 10 μM, whereas higher concentrations caused correspondingly larger decreases in [^{3}H]thymidine incorporation (Fig. 1*A*). To evaluate the potential for MEHP to induce apoptosis in primary bone marrow B cells, cells were treated at a range of MEHP concentrations (10–150 μM) for 16 h, stained with PI, and analyzed for the percentage of cells with a subG_0/G_1 DNA content. Apoptosis was readily detected by flow cytometry after exposure to MEHP (Fig. 1*B*). Treatment with doses as low as 25 μM MEHP consistently induced apoptosis in a significant fraction of these $B220^+/CD43^+$ B cells (Fig. 1*C*). The percentage of apoptotic cells increased with increasing concentrations of MEHP, reaching ~35% above background at 150 μM. These data are consistent with those obtained with PPARγ agonist drugs and suggest that environmental phthalates are similarly immunotoxic.

MEHP reduces [^{3}H]thymidine incorporation and induces apoptosis and cell cycle arrest in a pro/pre-B cell line

A nontransformed, bone marrow stromal cell-dependent pro/pre-cell line, BU-11, was used to confirm and extend studies on the

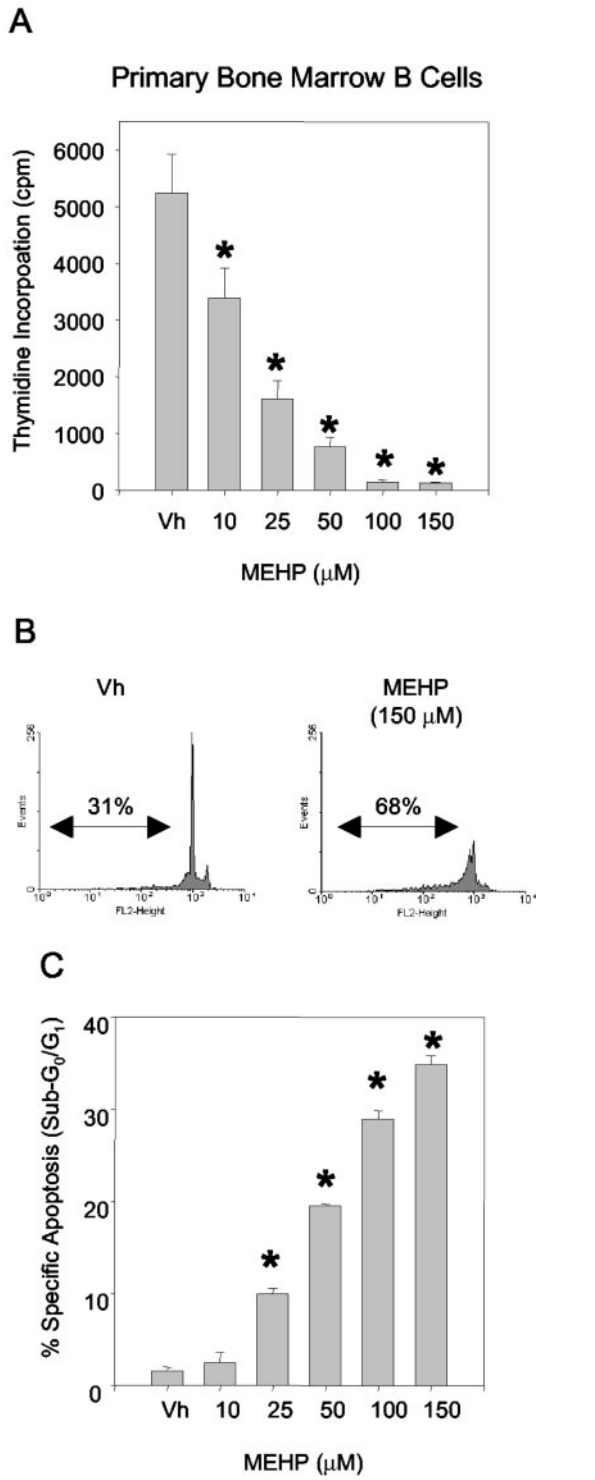

FIGURE 1. The phthalate metabolite MEHP suppresses [^{3}H]thymidine incorporation (*A*) and induces apoptosis (*B* and *C*) in primary bone marrow B cells. Primary bone marrow B cell populations (>95% B220$^+$/CD43$^+$) were prepared as described in *Materials and Methods*. Suspension cultures of primary bone marrow B cells were treated with ethanol (vehicle, <0.5%) or MEHP (10–150 μM) for 48 h ([^{3}H]thymidine; *A*) or 16 h (PI staining; *B* and *C*). [^{3}H]thymidine incorporation and apoptosis (formation of a subG$_0$/G$_1$ population after PI staining) were analyzed as described in *Materials and Methods*. The specific apoptosis was calculated by subtracting the background subG$_0$/G$_1$ population from each measurement from cells from that individual mouse. Data are presented as the mean ± SE from cultures derived from five to nine individual mice. ∗, Statistically different from vehicle-treated ($p <$ 0.01, by ANOVA and Dunnett's test).

effects of MEHP on developing B lymphocytes. First, BU-11 cells were exposed to increasing concentrations of MEHP, and [^{3}H]thymidine incorporation was assessed 48 h later to compare the responses of this cell line to those seen with primary B cells. As with primary bone marrow B cells, MEHP caused a significant reduction in [^{3}H]thymidine incorporation in BU-11 pro/pre-B cells (Fig. 2, open histograms), although BU-11 cells were less sensitive to the MEHP-dependent decrease in [^{3}H]thymidine incorporation than primary bone marrow B cells.

If inhibition of [^{3}H]thymidine incorporation were due to activation of PPARγ, it would be predicted that simultaneous activation of its dimerization partner, RXRα, would enhance the biological effect of MEHP. For example, cotreatment of cells with PPARγ and RXRα agonists results in enhanced PPRE-dependent transcription (18–21). Therefore, we tested the effect of MEHP and 9-*cis*-RA cotreatment on [^{3}H]thymidine incorporation by BU-11 cells. [^{3}H]thymidine incorporation was reduced significantly in BU-11 cells by treatment with 9-*cis*-RA (10 μM) alone (Fig. 2, first solid histogram). Importantly, cotreatment with 10 μM 9-*cis*-RA and MEHP potentiated the reduction of [^{3}H]thymidine incorporation by BU-11 cells (Fig. 2, solid histograms) at all MEHP concentrations.

A reduction in [^{3}H]thymidine incorporation can be attributable to a diminution of DNA synthesis (i.e., proliferation) and/or an increase in cell death. To distinguish between these two possibilities, BU-11 cells were stained with PI and analyzed by flow cytometry for the percentage of cells expressing a subG$_0$/G$_1$ fluorescence peak (i.e., apoptotic cells) and for the percentage of cells expressing S/G$_2$/M levels of DNA (i.e., dividing cells).

To evaluate the potential for MEHP to induce apoptosis, BU-11 cells were treated with 50–200 μM MEHP for 24 h. BU-11 cells exhibited a relatively low level of background apoptosis (<7%;

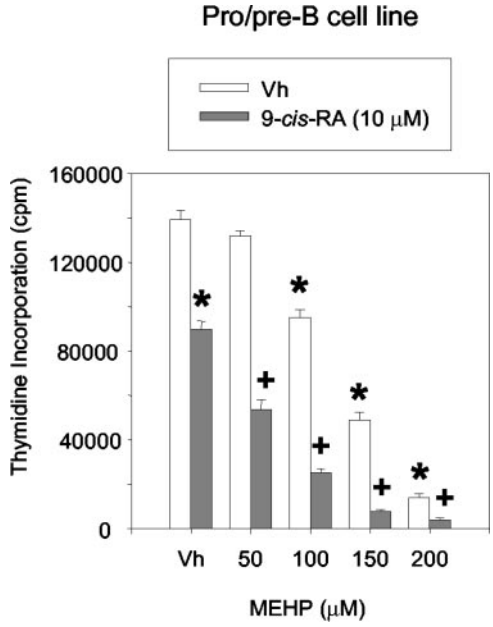

FIGURE 2. MEHP suppresses [^{3}H]thymidine incorporation in a nontransformed pro/pre-B cell line (BU-11). Suspension cultures of BU-11 cells were treated with ethanol (vehicle, 0.5%), MEHP (50–200 μM), and/or 9-*cis*-RA (10 μM) for 48 h. [^{3}H]thymidine incorporation was determined as described in *Materials and Methods*. Data are presented as the mean ± SE from four experiments. ∗, Statistically different from vehicle-treated ($p <$ 0.01, by ANOVA and Fisher's PLSD test). +, Statistically different from 9-*cis*-RA- and MEHP-treated at the same concentration ($p <$ 0.01, by ANOVA and Fisher's PLSD test).

Fig. 3, *A* and *B*). Treatment with 150 or 200 μM MEHP consistently induced apoptosis in a significant fraction of these pro/pre-B cells (~20 and ~40%, respectively). As expected, DNA fragmentation, a hallmark of apoptosis, was readily demonstrated in BU-11 cells after a 24-h exposure to 150–200 μM MEHP (Fig. 3*C*, *lanes 5* and *7*). Apoptosis also was confirmed by detection of poly(ADP-ribose) polymerase cleavage, an activity of effecter caspase 3, after exposure to 150–200 μM MEHP (data not shown).

To ascertain the contribution of RXRα to MEHP-induced apoptosis, BU-11 cells were treated with MEHP (50–200 μM) with or without 10 or 20 μM 9-*cis*-RA for 24 h. Addition of 10 or 20 μM 9-*cis*-RA to BU-11 cell cultures did not affect BU-11 cell viability (Fig. 3, *A* and *B*). In contrast, cotreatment with 20 μM 9-*cis*-RA and a suboptimal dose of MEHP, e.g., 100 μM, induced a significant level of apoptosis (Fig. 3*B*). Similarly, the 10 μM 9-*cis*-RA treatment significantly enhanced apoptosis induced by 150 μM MEHP (Fig. 3, *A* and *B*). Cotreatment with 20 μM 9-*cis*-RA and 150 μM MEHP increased the incidence of apoptosis even more (Fig. 3, *A* and *B*). The enhancement of apoptosis by 9-*cis*-RA in combination with MEHP also is reflected in DNA ladder formation (Fig. 3*C*, *lanes 5* and *6*). These data are consistent with a role for the PPARγ-RXRα heterodimer in MEHP-mediated pro/pre-B cell apoptosis signaling.

It was noted that BU-11 cell apoptosis could not be detected after exposure to 100 μM MEHP (Fig. 3, *B* and *C*), a concentration at which inhibition of [^{3}H]thymidine incorporation could be demonstrated (Fig. 2). Similarly, in primary bone marrow B cells, [^{3}H]thymidine incorporation was reduced significantly at concentrations below those at which apoptosis was evident (e.g., 10 μM; Fig. 1, *A* and *C*). These results suggest that MEHP induces growth arrest rather than apoptosis at low concentrations. To evaluate the potential for MEHP to induce growth arrest and thereby to reduce [^{3}H]thymidine incorporation, BU-11 cells were exposed to low concentrations of MEHP (50–100 μM) with and without 10 μM 9-*cis*-RA for 48 h.

A significant decrease in the number of cells in S/G_2/M was observed after treatment with 100 μM, but not 50 μM, MEHP (Fig. 4*A*, open histograms). Therefore, the reduction in [^{3}H]thymidine incorporation at 100 μM MEHP is probably due to growth arrest before or during the DNA synthesis phase. This decrease in

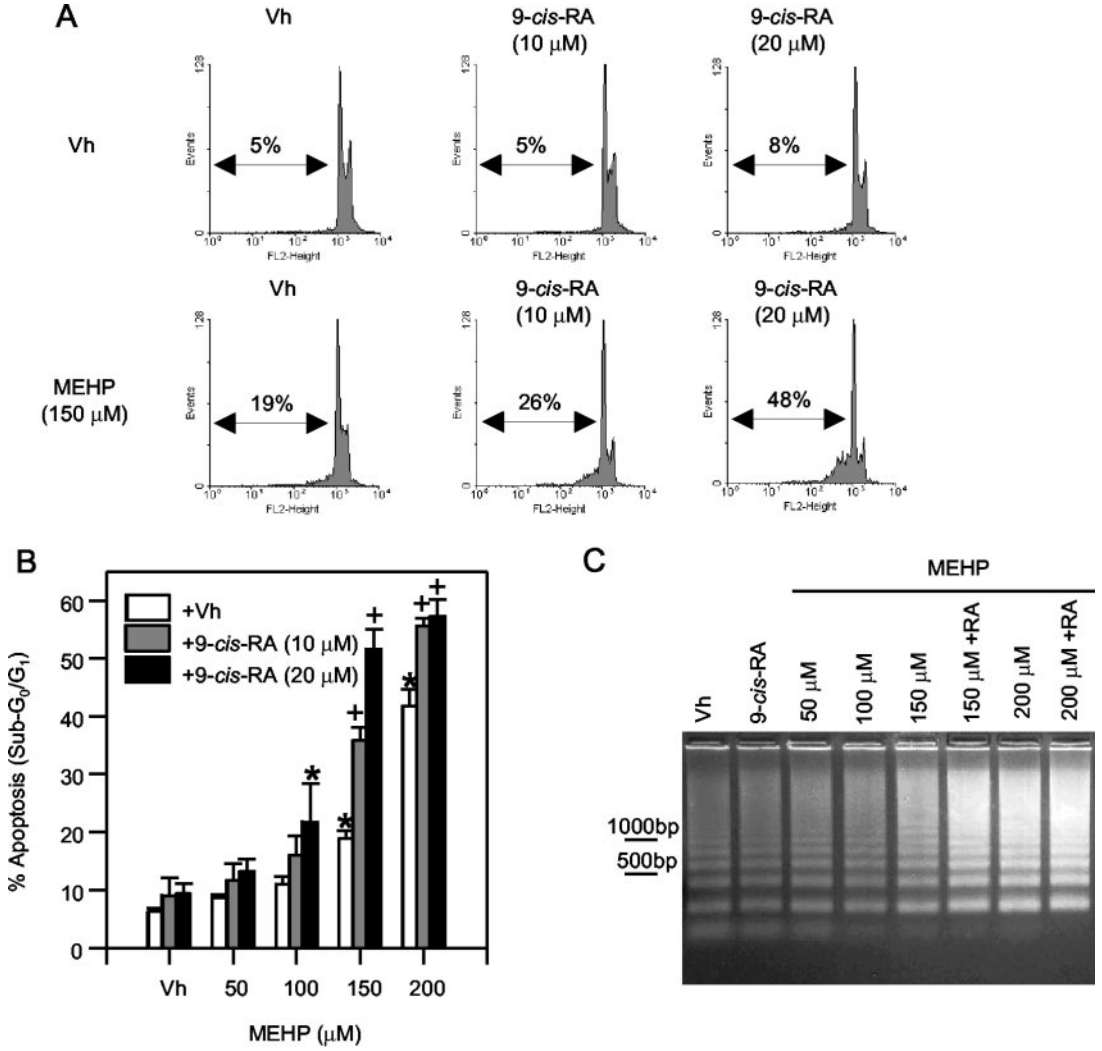

FIGURE 3. MEHP induces apoptosis in pro/pre-B cells. Suspension cultures of BU-11 cells were treated with ethanol (vehicle, 0.1%), MEHP (50–200 μM), and/or 9-*cis*-RA (10–20 μM) for 24 h. Apoptosis assays were performed as described in *Materials and Methods*. *A*, Formation of a subG_0/G_1 population after PI staining. Data are representative of four experiments. *B*, Quantification of the subG_0/G_1 population. Data are presented as the mean ± SE from four experiments. *, Statistically different from vehicle- and 9-*cis*-RA-treated ($p < 0.01$, by ANOVA and Fisher's PLSD test). +, Statistically different from vehicle-, 9-*cis*-RA-, and MEHP-treated at the same dose ($p < 0.01$, by ANOVA and Fisher's PLSD test). *C*, Formation of DNA ladders. Data are representative of three experiments.

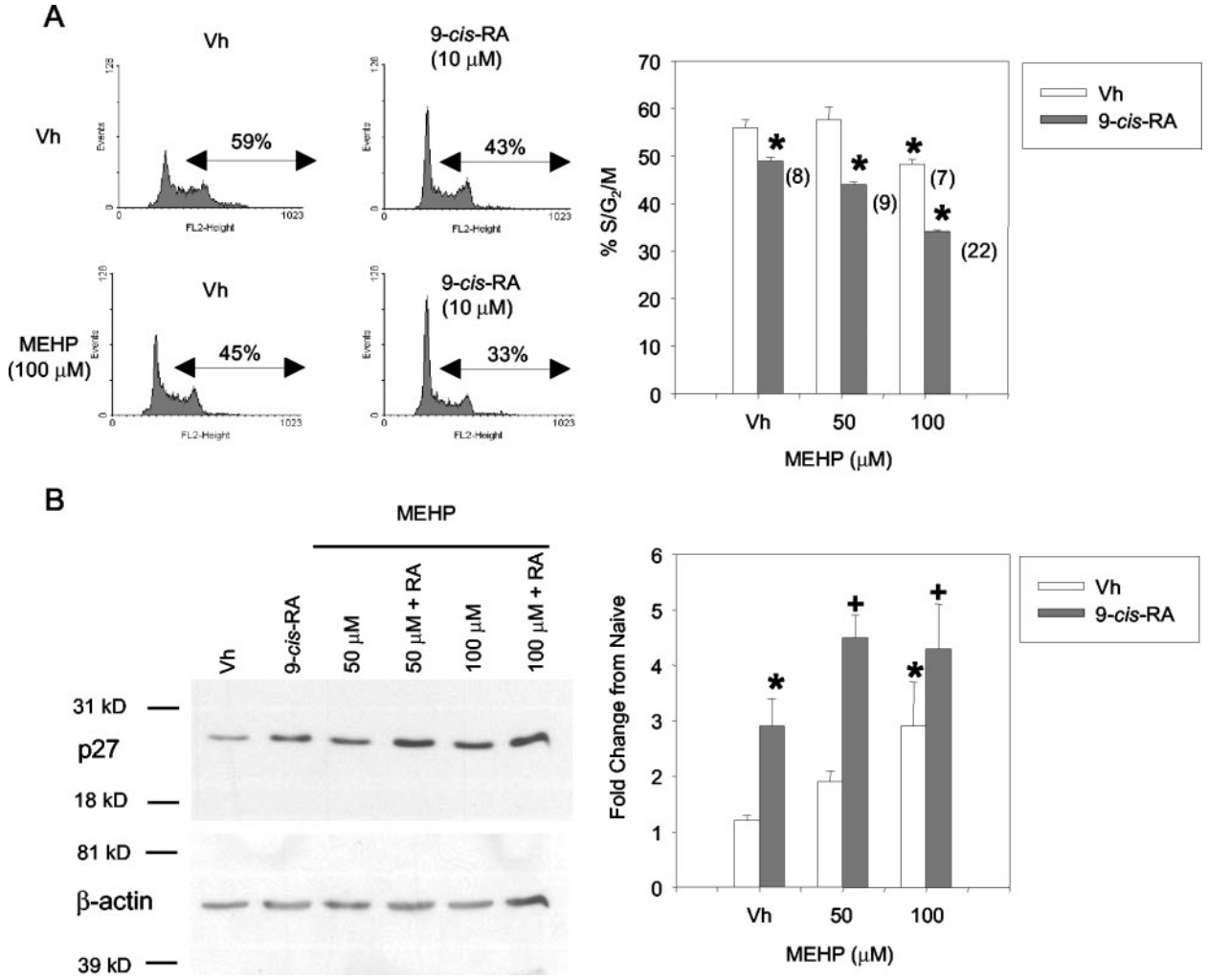

FIGURE 4. Low doses of MEHP induce cell cycle arrest in pro/pre-B cells. Suspension cultures of BU-11 cells were treated with ethanol (vehicle, 0.1%), MEHP (50–100 μM), and/or 9-*cis*-RA (10 μM) for 48 h. Assays were performed as described in *Materials and Methods*. *A*, Cell cycle distribution after PI staining. Data are presented as the mean ± SE from three experiments. ∗, Statistically different from vehicle-treated ($p < 0.05$, by ANOVA and Dunnett's test). *B*, $p27^{Kip1}$ expression. Data are presented as the mean ± SE from three experiments. ∗, Statistically different from vehicle-treated ($p < 0.05$, by ANOVA and Fisher's PLSD test). +, Significantly different from vehicle- and 9-*cis*-RA-treated ($p < 0.05$, by ANOVA and Fisher's PLSD test). There were no significant differences in β-actin expression.

the percentage of cycling cells was even more profound upon inclusion of 9-*cis*-RA (Fig. 4*A*, solid histograms). Although 10 μM 9-*cis*-RA or 100 μM MEHP alone reduced the percentage of cycling cells by 7–8%, the effects of treating cells with 10 μM 9-*cis*-RA together with 100 μM MEHP appeared more than additive (i.e., a 22% reduction in the percentage of cycling cells). Therefore, a PPARγ-RXRα complex appears to participate in growth arrest as it does in apoptosis induction.

The $p27^{Kip1}$ protein is a cyclin-dependent kinase inhibitor that blocks cyclin E/cyclin-dependent kinase 2, a cyclin that controls passage through G_1 into S phase (59). To begin to assess the mechanisms by which MEHP and 9-*cis*-RA induce cell cycle arrest, BU-11 cells were exposed to low concentrations of MEHP (50–100 μM) with and without 10 μM 9-*cis*-RA for 48 h. Whole-cell lysates were examined for $p27^{Kip1}$ expression by Western blotting. Treatment with either 100 μM MEHP or 9-*cis*-RA alone resulted in a modest, but statistically significant, increase in $p27^{Kip1}$ (Fig. 4*B*). As with the other readouts, the effects of 50 μM MEHP added together with 9-*cis*-RA were more profound than those with either agent alone (4.5-fold; $p < 0.05$). The results are consistent with the hypothesis that MEHP- and/or 9-*cis*-RA-mediated growth arrest involves the up-regulation of the cell cycle inhibitor $p27^{Kip1}$.

15d-PGJ$_2$, a natural PPARγ ligand in the bone marrow, reduces [^{3}H]thymidine incorporation by inducing apoptosis and cell cycle arrest in pro/pre-B lymphocytes

15d-PGJ_2 is a PPARγ agonist (44) whose precursor PGD_2 is found in high concentrations in the bone marrow microenvironment (43, 45), suggesting its role in lymphocyte development. As such, it may potentiate the toxic effects of environmental PPARγ agonists. To test this possibility, the ability of 15d-PGJ_2 to affect pro/pre-B cell growth and survival, either alone or in combination with MEHP, was evaluated.

BU-11 cells were exposed to increasing concentrations of 15d-PGJ_2 and 9-*cis*-RA for 48 h, and [^{3}H]thymidine incorporation was assessed. 15d-PGJ_2 caused a >90% reduction in [^{3}H]thymidine incorporation at concentrations as low as 5 μM (Fig. 5*A*). [^{3}H]thymidine incorporation was inhibited completely at ≥10 μM 15d-PGJ_2. Similarly, 5 μM 15d-PGJ_2 induced a significant increase in a subG_0/G_1 fluorescence peak after an 8-h exposure (vehicle, 10 ± 1%; 15d-PGJ_2, 62 ± 1%; $p < 0.01$) and significant DNA fragmentation after a 24-h exposure (Fig. 5*B*, *lane 5*). It is important to note that 2 μM 15d-PGJ_2 did not significantly affect either [^{3}H]thymidine incorporation or DNA fragmentation. These results

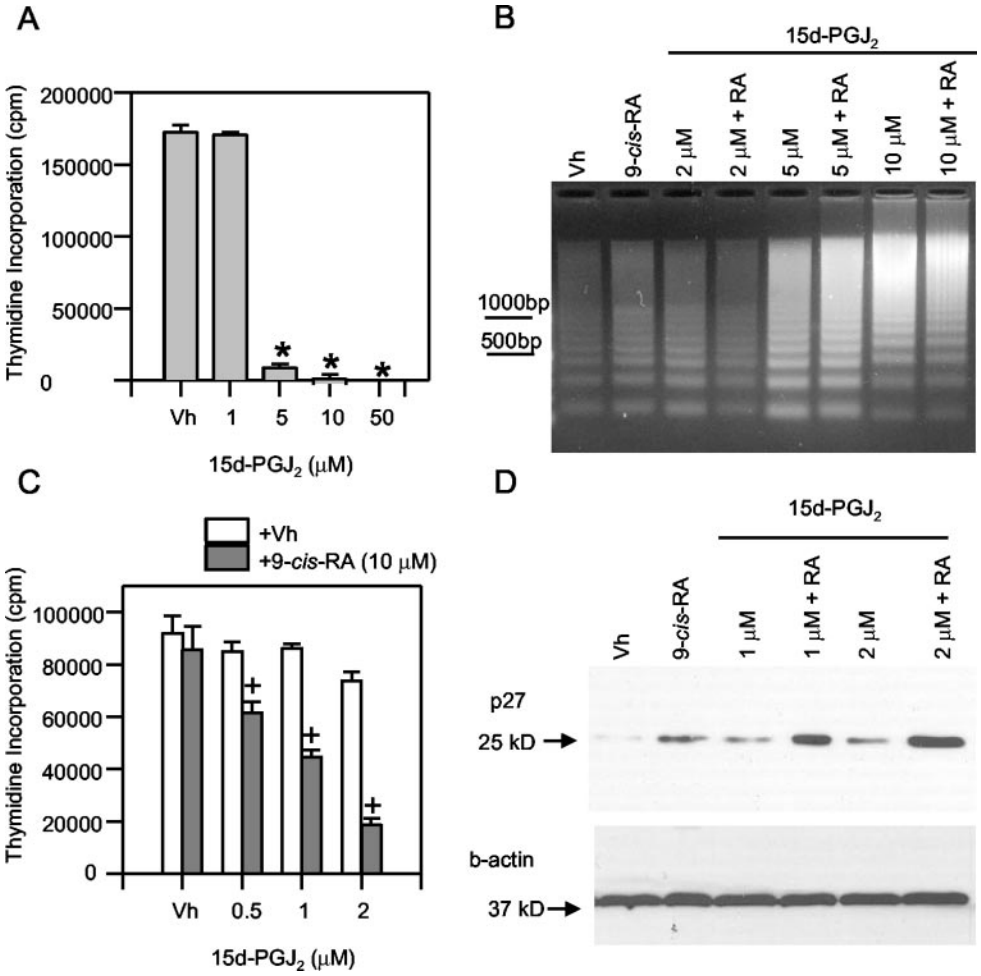

FIGURE 5. 15d-PGJ_2, a natural bone marrow-derived PPARγ ligand, inhibits [^{3}H]thymidine incorporation by inducing both apoptosis and cell cycle arrest in pro/pre-B cells. Suspension cultures of BU-11 cells were treated with ethanol (vehicle, <0.5%), 15d-PGJ_2 (0.5–50 μM), and/or 9-*cis*-RA (10 μM) for 24 h (DNA ladder formation) or 48 h ([^{3}H]thymidine incorporation and $p27^{kip1}$ expression). Assays were performed as described in *Materials and Methods*. A) [^{3}H]thymidine incorporation after treatment with 15d-PGJ_2. Data are presented as the mean ± SE from four experiments. ∗, Statistically different from vehicle-treated ($p < 0.01$, by ANOVA and Fisher's PLSD test). *B*, DNA ladder formation. Data are representative of three experiments. *C*, [^{3}H]thymidine incorporation after treatment with 15d-PGJ_2 and 9-*cis*-RA. Data are presented as the mean ± SE from four experiments. +, Statistically different from vehicle-, 9-*cis*-RA-, and 15d-PGJ_2-treated at the same dose ($p < 0.01$, by ANOVA and Fisher's PLSD test). *D*, $p27^{Kip1}$ expression. Data are representative of three experiments. Fold change from untreated cultures: vehicle, 1.1 ± 0.4; 15d-PGJ_2, 3.2 ± 1.0; 9-*cis*-RA, 9.0 ± 1.4; 15d-PGJ_2 and 9-*cis*-RA, 18.4 ± 4.0* (∗, statistically different from all other treatments ($p < 0.05$, by ANOVA and Fisher's PLSD test)). There were no significant differences in β-actin expression.

indicate that 15d-PGJ_2 is a potent inhibitor of pro/pre-B cell [^{3}H]thymidine uptake and that this decrease in [^{3}H]thymidine uptake is due, at least at concentrations ≥5 μM, to apoptosis induction.

Neither 10 μM 9-*cis*-RA nor 0.5 μM 15d-PGJ_2 had an effect on [^{3}H]thymidine incorporation when either agent was added alone (Fig. 5*C*). However, a combination of 10 μM 9-*cis*-RA and 0.5 μM 15d-PGJ_2 significantly reduced [^{3}H]thymidine incorporation (Fig. 5*C*, solid histograms). Indeed, the combinatorial effect of these respective PPARγ and RXRα agonists was most evident when adding 2 μM 15d-PGJ_2 together with 10 μM 9-*cis*-RA. However, no increase in DNA ladder formation was seen when combining 2 μM 15d-PGJ_2 and 10 μM 9-*cis*-RA (Fig. 5*B*), suggesting that the significant decrease in [^{3}H]thymidine incorporation was probably due to cell cycle arrest. Similarly, although 1–2 μM 15d-PGJ_2 or 10 μM 9-*cis*-RA alone increased $p27^{Kip1}$ expression, the combination of these respective PPARγ and RXRα agonists resulted in a significant effect with regard to $p27^{Kip1}$ expression (an 18.4 ± 4.0-fold increase; $p < 0.05$; Fig. 5*D*). Collectively, these data indicate that this natural PPARγ ligand induces $p27^{Kip1}$ expression concomitant with growth arrest at concentrations lower than those capable of inducing apoptosis (i.e., ≤2 μM) and that this effect is enhanced significantly by coactivation of a PPARγ dimerization partner, i.e., RXRa.

To determine whether 15d-PGJ_2 potentiates the activity of an environmental PPARγ agonist, BU-11 cells were treated with 100 μM MEHP, i.e., a suboptimal concentration that induces a low level of growth arrest (Fig. 4), but no apoptosis (Fig. 3), together with suboptimal concentrations of 15d-PGJ_2 (i.e., 1–2 μM; see Fig. 5). Interestingly, this combination resulted in a significantly greater reduction in [^{3}H]thymidine incorporation than seen with either PPARγ agonist alone (Fig. 6*A*). The enhanced loss of [^{3}H]thymidine incorporation with 100 μM MEHP and 1–2 μM 15d-PGJ_2 resulted from the induction of apoptosis, as evidenced by a significant increase in a subG_0/G_1 fluorescence peak (Fig. 6*B*) and an increase in DNA ladder formation (Fig. 6*C*).

Because apoptosis was induced after cotreatment with 100 μM MEHP and 15d-PGJ_2 (Fig. 6*B*), a lower MEHP dose, which does not induce apoptosis even in combination with 15d-PGJ_2 (i.e., 75

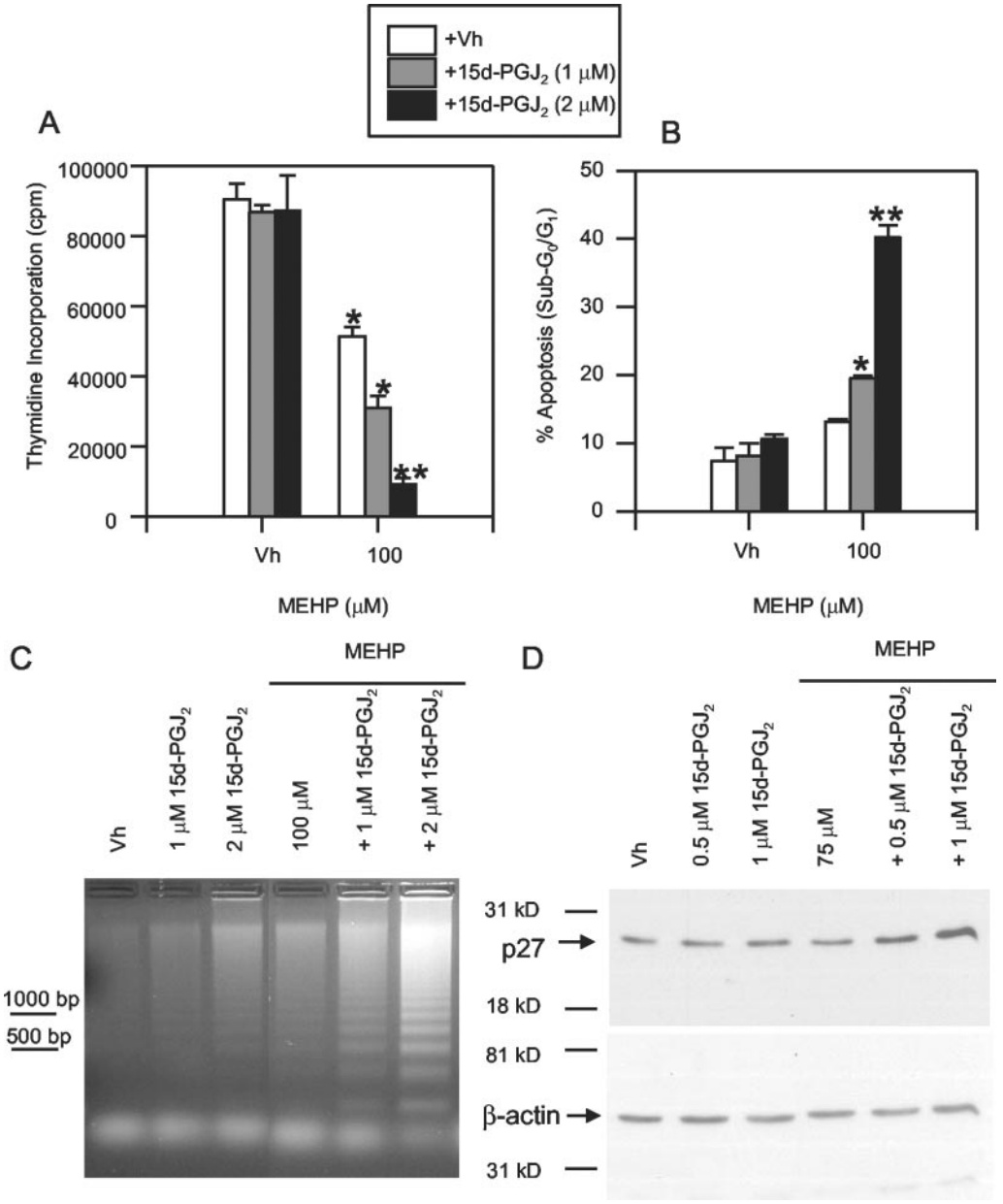

FIGURE 6. Cotreatment of pro/pre-B cells with 15d-PGJ_2 significantly enhances the MEHP-induced suppression of [^{3}H]thymidine incorporation. Suspension cultures of BU-11 were treated with ethanol (vehicle, <0.5%), MEHP (100 μM), and/or 15d-PGJ_2 (1–2 μM) for 24 h (PI staining and DNA ladder formation) or 48 h ([^{3}H]thymine incorporation and $p27^{kip1}$ expression). Assays were performed as described in *Materials and Methods*. *A*, [^{3}H]thymidine incorporation. *B*, Formation of a subG_0/G_1 population after PI staining. Data are presented as the mean ± SE from three experiments (*A* and *B*). ∗, Statistically different from vehicle-treated ($p < 0.01$, by ANOVA and Fisher's PLSD test). ∗∗, Statistically different from vehicle- and MEHP-treated at the same dose ($p < 0.01$, by ANOVA and Fisher's PLSD test). *C*, DNA ladder formation. Data are representative of three experiments. *D*, $p27^{Kip1}$ expression. Data are representative of three experiments. Fold change from naive: vehicle, 1.4 ± 0.1; 1 μM 15d-PGJ_2, 3.7 ± 0.8; 75 μM MEHP, 3.2 ± 0.5; 15d-PGJ_2 and MEHP, 8.2 ± 1.8* (∗, statistically different from all other treatments ($p < 0.01$, by ANOVA and Fisher's PLSD test)). There were no significant differences in β-actin expression.

μM), was used to assess $p27^{kip1}$ up-regulation, a marker for growth inhibition, in the presence of MEHP and 15d-PGJ_2. Suboptimal doses of either MEHP (75 μM) or 15d-PGJ_2 (0.5–1.0 μM) did not affect $p27^{Kip1}$ expression (Fig. 6*D*). However, a combination of these PPARγ ligands at these doses significantly increased $p27^{kip1}$ expression (Fig. 6*D*), a result consistent with a synergistic effect on growth inhibition. Considering that concentrations of 15d-PGJ_2 may be as high as the micromolar range in the bone marrow (43–45), these data suggest that even low exposures to environmental phthalates such as MEHP may have profound effects on bone marrow B cell growth and/or survival.

*Analyses of treatment with MEHP and 15d-PGJ_2 or 9-*cis*-RA; additive vs synergistic effects*

Although previous investigators have referred to the interaction of combinations of PPARγ/RXRα ligands as synergistic (18–21), the methodology used was not sufficient to distinguish true synergy from nonsynergistic, additive effects. The data presented in this study suggested a combinatorial effect between MEHP and 9-*cis*-RA or 15d-PGJ_2. Therefore, we used the isobole method to determine whether the enhancements in biological responses seen with treatment combinations were additive or synergistic. Contour

lines for the response surface of each combination were plotted. These contours represent levels of constant effect in the combination dose space, i.e., isoboles of effect. Isoboles of an asynergistic (i.e., concentration additive) interaction are represented by straight lines with negative slopes. Interactive combinations are manifest as isoboles which curve toward (synergism) or away from (antagonism) the origin (53, 54).

The isoboles of the MEHP plus 15d-PGJ_2 combination are nearly straight lines, indicating an effect that is at least additive effect (Fig. 7*A*). In contrast, the isoboles of the MEHP plus 9-*cis*-RA combination are more complex and across most of the concentration range curve toward the origin, indicating a strongly synergistic interaction in this region (Fig. 7*B*).

MEHP and 15d-PGJ_2 induce PPARγ-DNA binding and transcriptional trans-activation

MEHP has been shown in mouse embryonic carcinoma cells and in PPARγ-transfected COS cells to be a PPARγ agonist (15, 16).

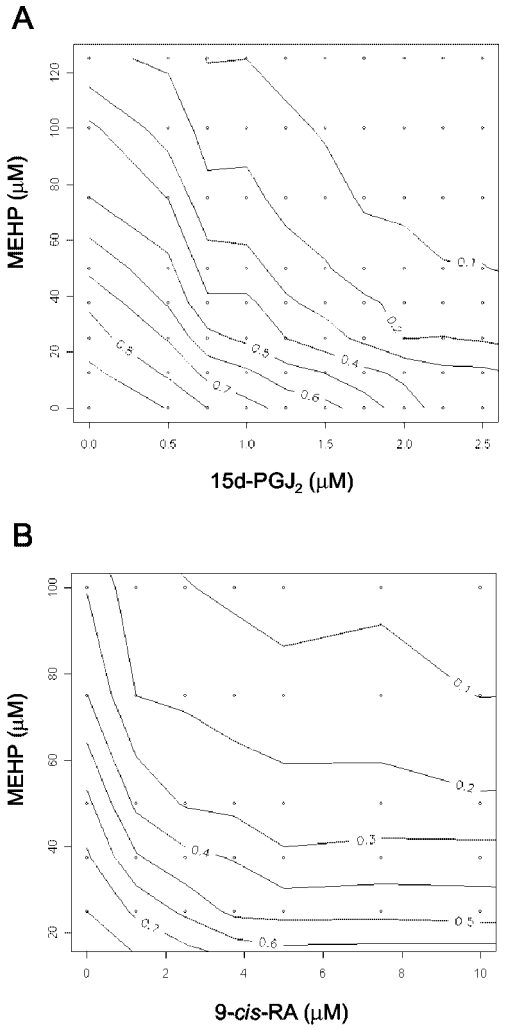

FIGURE 7. Isobole analysis of MEHP interactions with 15d-PGJ_2 (*A*) and 9-*cis*-RA (*B*). Suspension cultures of BU-11 cells were treated with ethanol (vehicle, 0.5%), MEHP (25–100 μM), 15d-PGJ_2 (0.5–2.5 μM), and/or 9-*cis*-RA (1–10 μM) for 48 h. [^{3}H]thymidine incorporation was determined, and contour plots (isobolograms) of the combinatorial effects of MEHP with 15d-PGJ_2 or 9-*cis*-RA were constructed as described in *Materials and Methods*. Levels shown are fractional responses of the Vh-Vh cell. Circles indicate locations of data points from three experiments. Contours are linear interpolation between points.

Previously we have shown that PPARγ, along with its dimerization partner, RXRα, are expressed at the pro/pre-B cell stage (31). Furthermore, the synergy between MEHP and 9-*cis*-RA seen in the present system is consistent with the activation of a PPARγ-RXR dimer. PPARγ-specific EMSAs were performed to confirm MEHP- and 15d-PGJ_2-induced PPARγ-DNA binding in pro/pre-B cells.

Treatment of BU-11 cells with MEHP or 15d-PGJ_2 increased binding to the PPRE sequence from the acyl-CoA oxidase gene (Fig. 8*A*). The presence of PPARγ in the DNA-binding complex was confirmed by a change in the banding pattern similar to that published previously (31) upon inclusion of a PPARγ-specific Ab (Fig. 8*A*). In addition, the band could be specifically competed by a 100-fold excess of unlabeled oligonucleotides containing PPREs, but not by DNA of an unrelated sequence. Interestingly, treatment of cells with a combination of suboptimal concentrations of MEHP and 15d-PGJ_2 resulted in PPRE-DNA binding greater than that of either compound alone (Fig. 8*A*). These results indicate that both MEHP and 15d-PGJ_2 induce PPARγ-DNA binding in these early B lymphocytes.

To compare MEHP-induced trans-activation with that induced by 15d-PGJ_2, COS-1 cells were transiently transfected with mouse PPARγ and with the luciferase reporter plasmid pHDx3-luc, containing three copies of a PPRE derived from the rat enoyl CoA hydratase/3-hydroxyacyl CoA promoter (Fig. 8*B*), or with the luciferase reporter plasmid pLuc-4A6−880, which included 880 nt of the 5′-flanking DNA of the PPARγ-responsive rabbit CYP4A6 gene (Fig. 8*C*). (Transient transfection of BU-11 cells with reporter constructs was not practical because of the high levels of death and the low transfection efficiency seen in these nontransformed cells after either electroporation or FuGene treatment.)

Treatment of transfected COS-1 cells under serum-free conditions with the potent PPARγ agonist, troglitazone (3 μM), as a positive control resulted in a 15-fold activation of the CoA reporter and a 6-fold activation of the CYP4A6 reporter (Fig. 8, *B* and *C*). MEHP (20 μM) stimulated a 7-fold activation of the CoA reporter construct and a 3-fold activation of the CYP4A6 reporter (Fig. 8*B*). Treatment with 1–5 μM 15d-PGJ_2 resulted in a concentration-dependent increase in activation of the CoA reporter construct, with a 15-fold increase in activation at 5 μm (Fig. 8*B*). In contrast, 15d-PGJ_2 exhibited weaker activation of the CYP4A6 reporter, requiring 15 μM 15d-PGJ_2 for only a 4-fold increase in activity (Fig. 8*C*). These results show that although MEHP has a lower potency and efficacy in trans-activating the hydroxylacyl CoA gene than 15-dPGJ_2, MEHP and 15d-PGJ_2 have similar potencies and efficacies in trans-activating the CYP4A6 gene.

Apoptosis induced by MEHP and 15d-PGJ_2 does not result from inhibition of NF-κB activation

Previous studies suggested that PPARγ activation can either enhance (60−62) or down-regulate (36, 37, 63–67) NF-κB activity, and that NF-κB down-regulation results in apoptosis (37). To determine the effect of endogenous and environmental PPARγ agonists on NF-κB activation, BU-11 cells were treated with 5 μM 15d-PGJ_2 for 2 h or with 200 μM MEHP for 8 h. Nuclear proteins were extracted and assayed by EMSA for binding to the upstream κB regulatory element of c-*myc*. Unlike some studies with 15d-PGJ_2 (36, 63), but consistent with our previous studies with PPARγ agonists (31), treatment with 15d-PGJ_2 increased NF-κB-DNA binding 1.7-fold ($p < 0.01$) at 2 h post-treatment (Fig. 9, *A* and *B*). The failure to detect a change in binding of the constitutively active Oct-1 transcription factor with its cognate DNA binding element confirmed the specificity of the NF-κB response (data not shown). Similarly, treatment with MEHP for 8 h resulted in a significant ($p < 0.01$) 1.5-fold increase in NF-κB-DNA binding.

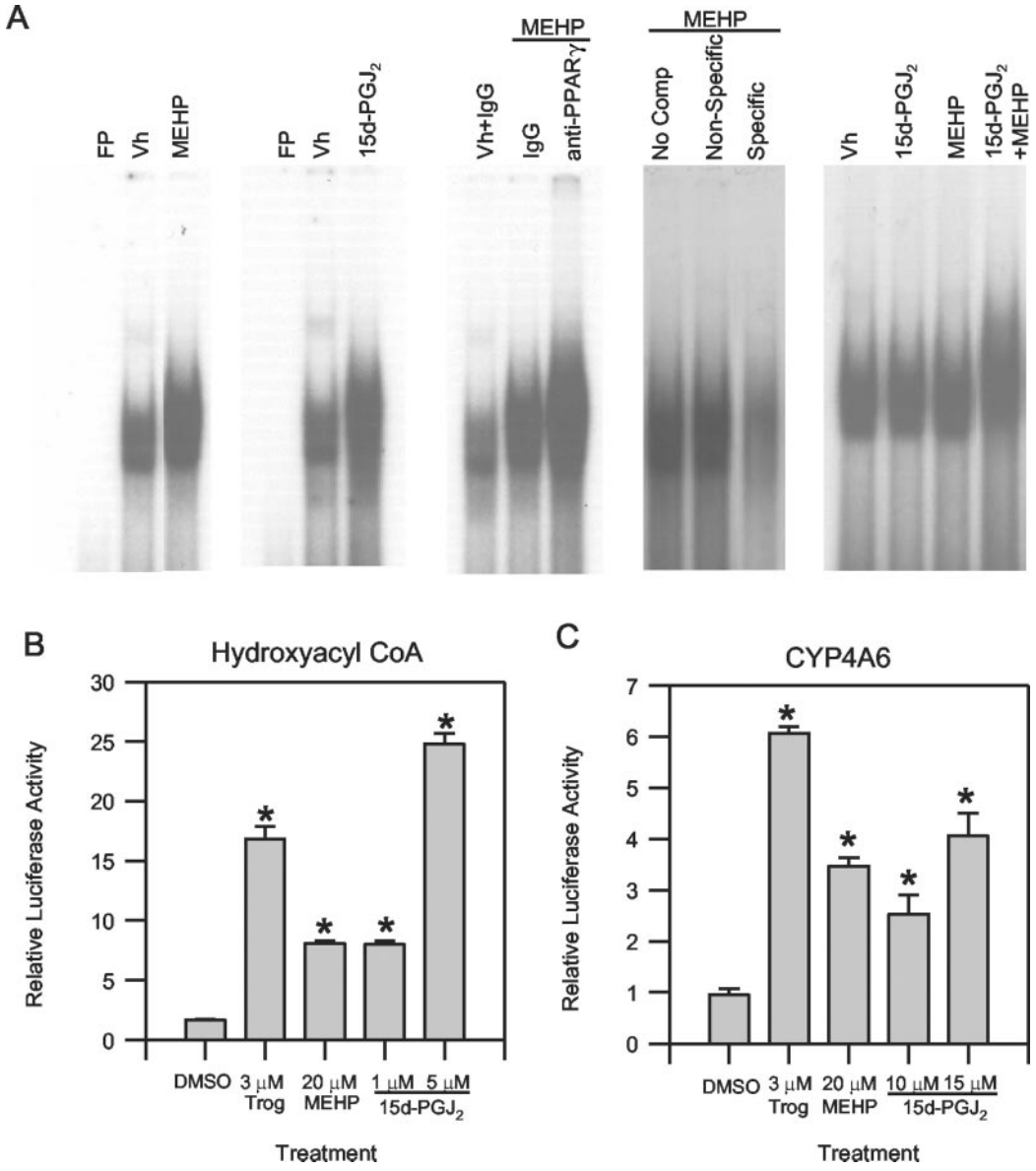

FIGURE 8. MEHP and 15d-PGJ_2 induce PPARγ-DNA binding and transcriptional transactivation. *A*, EMSA analysis of acyl CoA PPRE oligonucleotide binding. Nuclear extracts were prepared from BU-11 cells treated with ethanol (vehicle, 0.1%), MEHP (200 μM), or 15d-PGJ_2 (5 μM) for 24 h (*first four panels*) or with MEHP (100 μM) with or without 15d-PGJ_2 (2.5 μM) for 24 h (*last panel on the right*). EMSAs were performed as described in *Materials and Methods*. Supershift analyses were performed by including 2 μl of nonspecific rabbit IgG or polyclonal PPARγ-specific Ab. Competition analyses were performed by including a 100-fold excess of nonspecific or specific DNA. Similar results were found using nuclear extracts from 15d-PGJ_2-treated cells. FP, free probe. Data are representative of two or three experiments. *B* and *C*, Reporter analysis of PPARγ transactivation. COS-1 cells were transfected with reporters driven by the PPRE from the rat enoyl CoA hydratase/3-hydroxylacyl CoA promoter (*B*) or from the rabbit CYP4A6 promoter (*C*) as described in *Materials and Methods*. Luciferase activity was determined 24 h after treatment with DMSO (vehicle, 0.05%), MEHP (20 μM), 15d-PGJ_2 (1–15 μM), or troglitazone (3 μM) under serum-free conditions. Data represent PPARγ-driven firefly luciferase reporter activity normalized to CMV-driven control *Renilla* luciferase reporter activity and are presented as the mean $\pm$ SE from three experiments. $*$, Statistically different from vehicle-treated ($p < 0.01$, by ANOVA and Fisher's PLSD test).

Supershift assays then were used to identify the subunits in the active NF-κB complex. An Ab to p50 supershifted both the faster and slower migrating κB complexes (indicated by single and double arrows, respectively; Fig. 9*C*), whereas p65/RelA- and c-Rel-specific Abs significantly decreased the slower migrating κB band (double arrows above the dashed line). These results are similar to those obtained with the synthetic PPARγ ligands, ciglitazone and GW7845 (31). In general, these results indicate that, unlike apoptosis induced with other environmental chemicals (52), apoptosis induced in developing B cells by natural or environmental PPARγ ligands is not mediated by NF-κB down-regulation.

Discussion

Humans receive significant ambient daily exposures to phthalates and substantially higher acute exposures during medical procedures (68). It is increasingly apparent that these environmental phthalate exposures may have significant biological consequences. For example, exposure to one phthalate, DEHP, results in hepatocarcinogenesis (8) and renal, ovarian, testicular, and developmental toxicity (9–12). Similarly, MEHP, the active metabolite of DEHP, suppresses aromatase expression in a model of reproductive toxicity (13) and induces Fas-dependent

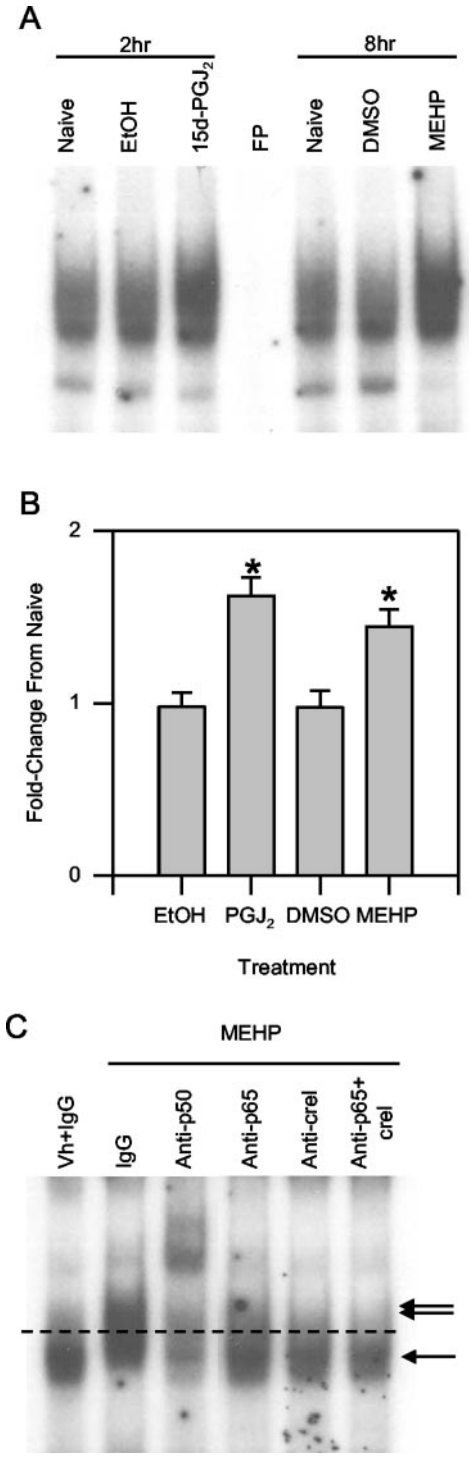

FIGURE 9. MEHP and 15d-PGJ_2 activate NF-κB-DNA binding in pro/pre-B cells. Nuclear extracts were prepared from BU-11 cells treated with ethanol (vehicle, 0.1%) or 15d-PGJ_2 (5 μM) for 2 h or from BU-11 cells treated with DMSO (vehicle, 0.01%) or MEHP (200 μM) for 8 h. Nuclear extracts were analyzed by EMSA for NF-κB oligonucleotide binding as described in *Materials and Methods*. *A*, NF-κB activation after treatment with 15d-PGJ_2 or MEHP. Data are representative of three experiments. *B*, Quantification of NF-κB-DNA binding. Data are presented as the mean ± SE from three experiments. ∗, Statistically different from vehicle-treated ($p < 0.01$, by Student's *t* test). *C*, Supershift analyses of NF-κB-DNA binding were performed by including 2 μl of polyclonal Ab specific for p50, p65/RelA, or c-Rel. The single arrow indicates the faster migrating p50:p50 complexes, and the double arrows above the dashed line indicate the slower migrating p50:p65 and p50:cRel complexes. Similar results were found using nuclear extracts from 15d-PGJ_2-treated cells (data not shown).

apoptosis in testis (10). Much of this toxicity is mediated by PPARγ or PPARγ together with PPARα (8, 9, 11, 26, 27).

The facts that phthalate ester metabolites are PPARγ agonists and that PPARγ agonist drugs induce lymphocyte apoptosis suggest that phthalate esters may target the immune system as well as those organ systems noted above. Several studies support this conclusion. Microarray analyses of liver from DEHP-treated C57BL/6 mice indicates down-regulation of complement components (69). High doses of MEHP and other monophthalates suppress OVA-specific Ab production in BALB/cJ mice (70). DEHP treatment of C57BL/6 mice induces severe thymic and splenic atrophy (71). In the spleen, treatment with another peroxisome proliferator, perfluoro-octanoic acid, decreases the total number of $CD19^+$ B cells by 86% and substantially reduces the percentage of splenic B cells (71). However, it is not clear whether this decrease is due to direct effects on mature B cell populations and/or on their development from bone marrow-derived precursors.

In this study we show for the first time that cells in the developing immune system indeed are sensitive to an environmental phthalate ester. MEHP both induces apoptosis and suppresses cell proliferation in developing bone marrow B cells. Considerable evidence supports a role for PPARγ in these processes: 1) pro/pre-B cells express PPARγ and RXRα (31); 2) cotreatment with MEHP and an RXRα agonist synergistically decreases cell growth and increases the incidence of apoptosis (Figs. 2–4 and 7); 3) MEHP induces binding of PPARγ complexes to PPAR-specific DNA responses elements (Fig. 8); and 4) MEHP induces PPRE-driven reporter activity (Fig. 8). The role of PPARγ in MEHP-induced pro/pre-B cell apoptosis is supported further by the fact that BU-11 cells are susceptible to apoptosis induced by synthetic PPARγ agonists (31). In addition, MEHP-induced apoptosis of U937 monocytic leukemia cells has been shown to be PPARγ dependent (72). However, these results do not preclude the possibility that PPARα-mediated processes contribute to the described effects (37).

Interestingly, cell cycle arrest occurred at MEHP concentrations lower than those required to induce apoptosis, effectively separating the two events. That is, no significant apoptosis induction was seen at 100 μM MEHP in BU-11 cells (Fig. 3), whereas 100 μM MEHP significantly reduced the percentage of cells in $S/G_2/M$ (Fig. 4). Similarly, a reduction in [^{3}H]thymidine, but no apoptosis induction, was seen in primary pro-B cells after exposure to 10 μM MEHP (Fig. 1). The increase in expression of $p27^{Kip1}$ in BU-11 cells suggests a role for this protein in MEHP-induced cell cycle arrest. Not surprisingly, cell cycle arrest is required for the PPARγ-mediated process of adipocyte terminal differentiation (73). Similarly, synthetic and natural PPARγ agonists can induce cell cycle arrest. For example, troglitazone induces p53, $p27^{Kip1}$, $p21^{Waf1}$, and Rb, while reducing cyclin D1 expression and cyclin-dependent kinase activity, resulting in G_1 arrest of hepatoma cells (74, 75). Similarly, troglitazone induces $p27^{Kip1}$ expression and G_1 cell cycle arrest in pancreatic carcinoma cells (76). Ciglitazone and 15d-PGJ_2 decrease cyclin D1 expression by enhancing its proteasome-dependent degradation, resulting in G_1 cell cycle arrest in MCF-7 breast cancer cells (77). Finally, ectopic expression of PPARγ in combination with pioglitazone treatment result in an early increase in $p27^{Kip1}$ and $p21^{Waf1}$ expression, followed by an increase in p18 expression and a loss of $p21^{Waf1}$ in fibroblasts (73). Collectively, these studies indicate that MEHP and other environmental PPARγ agonists may take advantage of a naturally occurring cell cycle arrest program in several cell types.

The analyses performed in this study suggest a strongly synergistic interaction between MEHP and 9-*cis*-RA in the induction of apoptosis (Fig. 7). Although synergistic induction of early B cell apoptosis and growth arrest by a combination of an environmental

PPARγ agonist and an RXRα activator has not been shown before, considerable precedent exists for increased signaling in other systems when both receptors are activated. The PPARγ/RXRα heterodimer is known as a permissive heterodimer in which RXRα ligands alone can activate transcription by the heterodimer (78). Cotreatment with ligands for both PPARγ and RXRα results in an increase in PPARγ-dependent transactivation of reporter genes, adipocyte differentiation in cultured cells (21), and differentiation of liposarcomas in vivo (79). The combinatorial effect results from increased recruitment of coactivators and an RXR-dependent conformational change in PPARγ (21).

Perhaps of still greater immunological significance is the effect seen when pro/pre-B cells were exposed to a combination of MEHP and an endogenous PPARγ ligand, 15d-PGJ_2 (Fig. 6). For example, cotreatment of pro/pre-B cells with 1–2 μM 15d-PGJ_2 and MEHP significantly reduced [^{3}H]thymidine incorporation and enhanced the growth arrest seen with MEHP alone. Furthermore, pro/pre-B cells underwent cell cycle arrest, but not apoptosis when treated with 1–2 μM 15d-PGJ_2 or 100 μM MEHP. However, when exposed to a combination of 2 μM 15d-PGJ_2 and 100 μM MEHP, considerable apoptosis was evident. Isobole analysis showed that this combinatorial effect was at least additive (Fig. 7*A*). Importantly, 15d-PGJ_2 and its precursor, PGD_2, are found at high concentrations in bone marrow, potentially reaching local concentrations in the micromolar range (43–45). These results suggest that B cells in the bone marrow microenvironment may be particularly susceptible to phthalate-induced toxicity. Indeed, because of the high background concentration of 15d-PGJ_2 in the bone marrow, the concentration of MEHP required to cause toxic effects in vivo may be significantly lower than those extrapolated from in vitro studies in which the effects of MEHP or other PPARγ agonists were studied in the absence of exogenous 15d-PGJ_2.

In summary, the results presented in this study demonstrate that an environmentally ubiquitous pollutant, DEHP/MEHP, is toxic to early bone marrow B cells and suggest that this immunotoxicity is at least in part PPARγ dependent. The developing B cell compartment is known to be exquisitely sensitive to other environmental toxins, such as polycyclic aromatic hydrocarbons (49, 57, 58). The sensitivity of primary bone marrow B cells is indicated by their significant response to concentrations of MEHP as low as 10 μM, a concentration 10-fold lower than that required to effect a response in the pro/pre-B cell line. Acute human exposure to DEHP/MEHP from a blood transfusion alone can be as high as 3–4 mg/kg for an adult weighing 70 kg (6), and concentrations in blood can range from 50–350 μM (7). Furthermore, the total daily ambient phthalate ester exposure of humans may reach 500 μg/kg/day (4). Considering that many phthalate esters are agonists for PPARs (13–16), that bone marrow contains high levels of a naturally occurring PG PPARγ agonist, and that primary bone marrow B cells have a relatively low threshold for phthalate-induced effects, the cumulative exposure to multiple phthalate esters may have significant consequences to developing human B lymphocytes. Further research is required to delineate the signaling pathways responsible for PPARγ agonist-induced B cells apoptosis.

References

1. Wams, T. J. 1987. Diethylhexylphthalate as an environmental contaminant: a review. *Sci. Total Env. 66:1*.
2. Blount, B. C., M. J. Silva, S. P. Caudill, L. L. Needham, J. L. Pirkle, E. J. Sampson, G. W. Lucier, R. J. Jackson, and J. W. Brock. 2000. Levels of seven urinary phthalate metabolites in a human reference population. *Env. Health Persp. 108:979*.
3. David, R. M. 2000. Exposure to phthalate esters. *Env. Health Perspect. 108: A440*.
4. Kohn, M. C., F. Parham, S. A. Masten, C. J. Portier, M. D. Shelby, J. W. Brock, and L. L. Needham. 2000. Human exposure estimates for phthalates. *Env. Health Perspect. 108:A440*.
5. Koch, H. M., H. Drexler, and J. Angerer. 2003. An estimation of the daily intake of di(2-ethylhexyl)phthalate (DEHP) and other phthalates in the general population. *Int. J. Hyg. Environ. Health 206:77*.
6. Center for the Evaluation of Risks to Human Reproduction. 2000. *NTP-CERHR Expert Panel Report on Di(2-ethylhexyl)phthalate*. Science International, Alexandria.
7. Plonait, S. L., H. Nau, R. F. Maier, W. Wittfoht, and M. Obladen. 1993. Exposure of newborn infants to di-(2-ethylhexyl)-phthalate and 2-ethylhexanoic acid following exchange transfusion with polyvinylchloride catheters. *Transfusion 33:598*.
8. Ward, J. M., J. M. Peters, C. M. Perella, and F. J. Gonzalez. 1998. Receptor and nonreceptor-mediated organ-specific toxicity of di(2-ethylhexyl)phthalate (DEHP) in peroxisome proliferator activated receptor α-null mice. *Toxicol. Pathol. 26:240*.
9. Lovekamp-Swan, T., and B. J. Davis. 2003. Mechanisms of phthalate ester toxicity in the female reproductive system. *Environ. Health Perspect. 111:139*.
10. Giammona, C. J., P. Sawhney, Y. Chandrasekaran, and J. H. Richburg. 2002. Death receptor response in rodent testis after mono-(2-ethylhexyl) phthalate exposure. *Toxicol. Appl. Pharmacol. 185:119*.
11. Park, J. D., S. S. Habeebu, and C. D. Klaassen. 2002. Testicular toxicity of di-(2-ethylhexyl)phthalate in young Sprague-Dawley rats. *Toxicology 171:105*.
12. Tomita, I., Y. Nakamura, Y. Yagi, and K. Tutikawa. 1986. Fetotoxic effects of mono-2-ethyhexyl phthalate (MEHP) in mice. *Environ. Health Perspect. 65:249*.
13. Lovekamp-Swan, T., A. M. Jetten, and B. J. Davis. 2003. Dual activation of PPARα and PPARγ by mono-(2-ethylhexyl)phthalate in rat ovarian granulosa cells. *Mol. Cell. Endocrinol. 201:133*.
14. Hurst, C. H., and D. J. Waxman. 2003. Activation of PPARα and PPARγ by environmental phthalate monoesters. *Toxicol. Sci. 74:297*.
15. Lampen, A., S. Zimnik, and H. Nau. 2003. Teratogenic phthalate esters and metabolites activate the nuclear receptors PPARs and induce differentiation of F9 cells. *Toxiol. Appl. Pharmacol. 188:14*.
16. Maloney, E. K., and D. J. Waxman. 1999. Trans-activation of PPARα and PPARγ by structurally diverse environmental chemicals. *Toxicol. Appl. Pharmacol. 161:209*.
17. Muerhoff, A. S., K. J. Griffin, and R. F. Johnson. 1992. The peroxisome proliferator-activated receptor mediates the induction of CYP4A6, a cytochrome P450 fatty acid omega-hydroxylase, by clofibric acid. *J. Biol. Chem. 267:19051*.
18. Kliewer, S. A., K. Umesono, D. J. Noonan, R. A. Heyman, and R. M. Evans. 1992. Convergence of 9-cis-retinoic acid and peroxisome proliferator signaling pathways through heterodimer formation of their receptors. *Nature 358:771*.
19. Keller, H., C. Dreyer, J. Medin, A. Mahfoudi, K. Ozato, and W. Wahli. 1993. Fatty acids and retinoids control lipid metabolism through activation of peroxisome proliferator-activated receptor-retinoid X receptor heterodimers. *Proc. Natl. Acad. Sci. USA 90:2160*.
20. Gearing, K. L., M. Gottlicher, M. Teboul, E. Widmark, and J. A. Gustafsson. 1993. Interaction of the peroxisome-proliferator-activated receptor and retinoid X receptor. *Proc. Natl. Acad. Sci. USA 90:1440*.
21. Schulman, I. G., G. Shao, and R. A. Heyman. 1998. Transactivation by retinoid X receptor-peroxisome proliferators-activated receptor (PPARγ) heterodimers: intermolecular synergy requires only the PPARγ hormone-dependent activation function. *Mol. Cell. Biol. 18:3483*.
22. Berger, J., and D. E. Moller. 2002. The mechanisms of action of PPARs. *Annu. Rev. Med. 53:409*.
23. Jones, D. C., X. Ding, and R. A. Daynes. 2002. Nuclear receptor PPARα is expressed in resting murine lymphocytes: the PPARα in T and B lymphocytes is both transactivation and transrepression competent. *J. Biol. Chem. 277:6836*.
24. Gonzalez, F. J. 2002. The peroxisome proliferator-activated receptor α (PPARα): role in hepatocarcinogenesis. *Mol. Cell. Endocrinol. 193:71*.
25. Yang, Q., Y. Xie, S. E. Alexson, B. D. Nelson, and J. W. DePierre. 2002. Involvement of the peroxisome proliferator-activated receptor α in the immunomodulation caused by peroxisome proliferators in mice. *Biochem. Pharmacol. 63:1893*.
26. Peters, J. M., M. W. Taubeneck, C. L. Keen, and F. J. Gonzalez. 1997. Di(2-ethylhexyl) phthalate induces a functional zinc deficiency during pregnancy and teratogenesis that is independent of peroxisome proliferator-activated receptor-α. *Teratology 56:311*.
27. Li, H., and K. H. Kim. 2003. Effects of mono-(2-ethylhexyl) phthalate on fetal and neonatal rat testis organ cultures. *Biol. Reprod. 69:1964*.
28. Greene, M. E., J. Pitts, M. A. McCarville, X. S. Wang, J. A. Newport, C. Edelstein, F. Lee, S. Ghosh, and S. Chu. 2000. PPARγ. Observations in the hematopoietic system. *Prostaglandin Lipid Mediators 62:45*.
29. Braissant, O., F. Foufelle, C. Scotto, M. Dauca, and W. Wahli. 1996. Differential expression of peroxisome proliferator-activated receptors: tissue distribution of PPARα, β and γ in the adult rat. *Endocrinology 137:453*.
30. Padilla, J., K. Kaur, C. H. J., T. J. Smith, and R. P. Phipps. 2000. Peroxisome proliferator activator receptor-γ agonists and 15-deoxy-$\Delta^{12,14}$-PGJ_2 induce apoptosis in normal and malignant B-lineage cells. *J. Immunol. 165:6941*.
31. Schlezinger, J. J., B. A. Jensen, K. K. Mann, H.-Y. Ryu, and D. H. Sherr. 2002. Peroxisome proliferator-activated receptor γ-mediated NF-κB activation and apoptosis in pre-B cells. *J. Immunol. 169:6831*.
32. Elbrecht, A., Y. Che, C. A. Cullinan, N. Hayes, M. D. Leibowitz, D. E. Moller, and J. Berger. 1996. Molecular cloning, expression and characterization of human peroxisome proliferator activated receptors γ1 and γ2. *Biochem. Biophys. Res. Commun. 224:431*.
33. Mueller, E., S. Drori, A. Aiyer, J. Yie, P. Sarraf, H. Chen, S. Hauser, E. D. Rosen, K. Ge, R. G. Roeder, and B. M. Spiegelman. 2002. Genetic analysis of adipogenesis through peroxisome proliferator-activated receptor γ isoforms. *J. Biol. Chem. 277:41925*.

34. Brown, K. K., B. R. Henke, S. G. Blanchard, J. E. Cobb, R. Mook, I. Kaldor, S. A. Kliewer, J. M. Lehmann, J. M. Lenhard, W. W. Harrington, et al. 1999. A novel *N*-aryl tyrosine activator of peroxisome proliferator-activated receptor-γ reverses the diabetic phenotype of the Zucker diabetic fatty rat. *Diabetes 48:1415*.
35. Jiang, C., A. T. Ting, and B. Seed. 1998. PPAR-γ agonists inhibit production of monocyte inflammatory cytokines. *Nature 391:82*.
36. Ricote, M., A. C. Li, T. M. Willson, C. J. Kelly, and C. K. Glass. 1998. The peroxisome proliferator activated receptor-γ is a negative regulator of macrophage activation. *Nature 391:79*.
37. Chinetti, G., S. Griglio, M. Antonucci, I. P. Torra, P. Delerive, Z. Majd, J. C. Fruchart, J. Chapman, J. Najib, and B. Staels. 1998. Activation of peroxisome proliferator-activated receptors α and γ induces apoptosis of human monocyte-derived macrophages. *J. Biol. Chem. 273:25573*.
38. Yang, X. Y., L. H. Wang, T. Chen, D. R. Hodge, J. H. Resau, L. DaSilva, and W. L. Farrar. 2000. Activation of human T lymphocytes is inhibited by peroxisome proliferator-activated receptor γ (PPARγ) agonists. *J. Biol. Chem. 275: 4541*.
39. Clark, R. B., D. Bishop-Bailey, T. Estrada-Hernandez, T. Hla, L. Puddington, and S. J. Padula. 2000. The nuclear receptor PPARγ and immunoregulation: PPARγ mediates inhibition of helper T cell responses. *J. Immunol. 164:1364*.
40. Gosset, P., A.-S. Charbonnier, P. Delerive, J. Fontaine, B. Staels, J. Pestel, A.-B. Tonnel, and F. Trottein. 2001. Peroxisome proliferator-activated receptor-γ activators affect the maturation of human monocyte-derived dendritic cells. *Eur. J. Immunol. 31:2857*.
41. Setoguchi, K., Y. Misaki, Y. Terauchi, T. Yamauchi, K. Kawahata, T. Kadowaki, and K. Yamamoto. 2001. Peroxisome proliferator-activated receptor-γ haploinsufficiency enhances B cell proliferative responses and exacerbates experimentally induced arthritis. *J. Clin. Invest. 108:1667*.
42. Harris, S. G., and R. P. Phipps. 2001. The nuclear receptor PPARγ is expressed by mouse T lymphocytes and PPARγ agonists induce apoptosis. *Eur. J. Immunol. 31:1098*.
43. Ujihara, M., Y. Urade, N. Eguchi, H. Hayashi, K. Ikai, and O. Hayaishi. 1988. Prostaglandin D_2 formation and characterization of its synthetases in various tissues of adult rat. *Arch. Biochem. Biophys. 260:521*.
44. Forman, B. M., P. Tontonoz, J. Chen, R. P. Brun, B. M. Spiegelman, and R. M. Evans. 1995. 15-Deoxy-$\Delta^{12,14}$-prostaglandin J_2 is a ligand for the adipocyte determination factor PPAR. *Cell 83:803*.
45. Fukushima, M. 1992. Biological activities and mechanisms of action of PGJ_2 and related compounds: an update. *Prostaglandins Leukotrienes Essen. Fatty Acids 47:1*.
46. Zhu, Y., K. Alvares, Q. Huang, M. S. Rao, and J. K. Reddy. 1993. Cloning of a new member of the peroxisome proliferator-activated receptor gene family from mouse liver. *J. Biol. Chem. 168:26817*.
47. Marcus, S. L., K. S. Miyata, B. Zhang, S. Subramani, R. A. Rachubinski, and J. P. Capone. 1993. Diverse peroxisome proliferator-activated receptors bind to the peroxisome proliferator-responsive elements of the rat hydratase/dehydrogenase and fatty acyl-CoA oxidase genes but differentially induce expression. *Proc. Natl. Acad. Sci. USA 90:5723*.
48. Tze, L. E., E. A. Baness, K. L. Hippen, and T. W. Behrens. 2000. Ig light chain receptor editing in anergic B cells. *J. Immunol. 165:6796*.
49. Mann, K., R. Matulka, M. Hahn, A. Trombino, B. Lawrence, N. Kerkvliet, and D. Sherr. 1999. The role of polycyclic aromatic hydrocarbon metabolism in dimethylbenzanthracene-induced pre-B lymphocyte apoptosis. *Toxicol. Appl. Pharmacol. 161:10*.
50. Hardy, R. R., C. E. Carmack, S. A. Shinton, J. D. Kemp, and K. Hayakaya. 1991. Resolution and characterization of pro-B and pre-pro-B cell stages in normal mouse bone marrow. *J. Exp. Med. 173:1213*.
51. Pietrangeli, C., S.-I. Hayashi, and P. Kincade. 1988. Stromal cell lines which support lymphocyte growth: characterization, sensitivity to radiation and responsiveness to growth factors. *Eur. J. Immunol. 18:863*.
52. Ryu, H.-Y., K. Mann, J. Schlezinger, B. Jensen, and D. Sherr. 2003. Environmental chemical-induced pro/pre-B cell apoptosis: analysis of c-Myc, p27(Kip1), and p21(WAF1) reveals a death pathway distinct from clonal deletion. *J. Immunol. 170:4897*.
53. Greco, W. R., G. Bravo, and J. C. Parsons. 1995. The search for synergy: a critical review from a response surface perspective. *Pharmacol. Rev. 47:331*.
54. Berenbaum, M. C. 1989. What is synergy? *Pharmacol. Rev. 41:93*.
55. Juge-Abury, C., A. Pernin, T. Favex, A. Burger, W. Wahl, C. A. Meier, and B. Desvergne. 1997. DNA binding properties of peroxisome proliferators-activated receptor subtypes on various natural peroxisome proliferators response elements. *J. Biol. Chem. 272:25252*.
56. Duyao, M. P., A. J. Buckler, and G. E. Sonenshein. 1990. Interaction of an NF-κB-like factor with a site upstream of the *c-myc* promoter. *Proc. Natl. Acad. Sci. USA 87:4727*.
57. Holladay, S. D., and B. J. Smith. 1994. Fetal hematopoietic alterations after maternal exposure to benzopyrene: a cytometric evaluation. *J. Toxicol. Environ. Health 42:259*.
58. Thurmond, L. M., J. E. Staples, A. E. Silverstone, and T. A. Gasciewicz. 2000. The aryl hydrocarbon receptor has a role in the in vivo maturation of murine bone marrow B lymphocytes and their response to 2,3,7,8-tetrachlorodibenzo-*p*-dioxin. *Toxicol. Appl. Pharmacol. 165:227*.
59. Slingerland, J., and M. Pagano. 2000. Regulation of the cdk inhibitor p27and is deregulation in cancer. *J. Cell. Physiol. 183:10*.
60. Coutureir, C., A. Brouillet, C. Couriaud, K. Koumanov, G. Bereziat, and M. Andreani. 1999. Interleukin 1β induces type II-secreted phospholipase A_2 gene in vascular smooth muscle cells by a nuclear factor κB and peroxisome proliferator-activated receptor-mediated process. *J. Biol. Chem. 274:23085*.
61. Ikawa, H., H. Kameda, H. Kamitani, S. J. Baek, J. B. Nixon, L. C. Hsi, and T. E. Eling. 2001. Effect of PPAR activators on cytokine-stimulated cyclooxygenase-2 expression in human colorectal carcinoma cells. *Exp. Cell Res. 267:73*.
62. Sun, Y. X., H. T. Wright, and S. Janciasukiene. 2002. α1-Antichymotrypsin/Alzheimer's peptide Aβ(1–42) complex perturbs lipid metabolism and activates transcription factors PPARγ and NFκB in human neuroblastoma (Kelly) cells. *J. Neurosci. Res. 67:511*.
63. Straus, D. S., G. Pascual, M. Li, J. S. Welch, M. Ricote, C.-H. Hsiang, L. L. Sengchanthalangsy, G. Ghosh, and C. K. Glass. 2000. 15-Deoxy-$\Delta^{12,14}$-prostaglandin J_2 inhibits multiple steps in the NF-κB signaling pathway. *Proc. Natl. Acad. Sci. USA 97:4844*.
64. Uchimura, K., M. Nakamuta, M. Enjoji, T. Irie, R. Sugimoto, T. Muta, H. Iwamoto, and H. Nawata. 2001. Activation of retinoic X receptor and peroxisome proliferator-activated receptor-γ inhibits nitric oxide and tumor necrosis factor-α production in rat Kupffer cells. *Hepatology 33:91*.
65. Chung, S. W., B. Y. Kang, S. H. Kim, Y. M. Kim, D. Cho, G. Trinchieri, and T. S. Kim. 2000. Oxidized low density lipoprotein inhibits interleukin 12 production in lipopolysaccharide-activated mouse macrophages via direct interaction between PPAR γ and NF-κB. *J. Biol. Chem. 276:32681*.
66. Ji, J. D., H. Cheon, J. B. Jun, S. J. Choi, Y. R. Kim, Y. H. Lee, T. H. Kim, I. J. Chae, G. G. Song, D. H. Yoo, et al. 2001. Effects of peroxisome proliferator-activated receptor-γ (PPAR-γ) on the expression of inflammatory cytokines and apoptosis induction in rheumatoid synovial fibroblasts and monocytes. *J. Autoimmun. 17:215*.
67. Gupta, R. A., D. B. Polk, U. Krishna, D. A. Israel, F. Yan, R. N. DuBois, and R. M. Peek, Jr. 2001. Activation of peroxisome proliferator-activated receptor γ suppresses nuclear factor κB-mediated apoptosis induced by *Helicobacter pylori* in gastric epithelial cells. *J. Biol. Chem. 276:31059*.
68. Tickner, J. A., T. Schettler, T. Guidotti, M. McCally, and M. Rossi. 2001. Health risks posed by use of di-2-ethylhexyl phthalate (DEHP) in PVC medical devices: a critical review. *Am. J. Ind. Med. 39:100*.
69. Wong, J. S., and S. S. Gill. 2002. Gene expression changes induced in mouse liver by di(2-ethylhexyl)phthalate. *Toxicol. Appl. Pharmacol. 185:180*.
70. Larsen, S. T., J. S. Hansen, P. Thygesen, M. Begtrup, O. M. Poulsen, and G. D. Nielsen. 2001. Adjuvant and immuno-suppressive effect of six monophthaltes in a subcutaneous injection model with BALB/c mice. *Toxicology 169:37*.
71. Yang, Q., Y. Xie, and W. Depierre. 2001. Effects of peroxisome proliferators on the thymus and spleen of mice. *Clin. Exp. Immunol. 122:219*.
72. Yokoyama, Y., T. Okubo, I. Kano, S. Sato, and K. Kano. 2003. Induction of apoptosis by mono(2-ethylhexyl)phthalate (MEHP) in U937 cells. *Toxciol. Lett. 144:371*.
73. Morrison, R. F., and S. R. Farmer. 1999. Role of PPARγ in regulating a cascase expression of cyclin-dependent kinase inhibitors, p18(INK4c) and p21(Waf1/Cip1), during adipogenesis. *J. Biol. Chem. 274:17088*.
74. Yoshizawa, K., D. P. Cioca, S. Kawa, E. Tanaka, and K. Kiyosawa. 2002. Peroxisome proliferator-activated receptor γ ligand troglitazone induces cell cycle arrest and apoptosis of hepatocellular carcinoma cell lines. *Cancer 95:2243*.
75. Brae, M. A., H. Rhee, and B. J. Song. 2003. Troglitazone but not rosiglitazone induces G_1 cell cycle arrest and apoptosis in human and rat hepatoma cell lines. *Toxicol. Lett. 139:67*.
76. Motomura, W., T. Okomura, N. Takahashi, T. Obara, and Y. Kohgo. 2000. Activation of peroxisome proliferator-activated receptor γ by troglitazone inhibits cell growth through the increase in p27 Kip1 in human pancreatic carcinoma cells. *Cancer Res. 60:5558*.
77. Qin, C., R. Burghardt, R. Smith, M. Wormke, J. Stewart, and S. Safe. 2003. Peroxisome proliferator-activated receptorγ agonists induce proteasome-dependent degradation of cyclin D1 and estrogen receptorα in MCF-7 breast cancer cells. *Cancer Res. 63:958*.
78. Leblanc, B. P., and H. G. Stunnenberg. 1995. 9-*cis* retinoic acid signaling: changing partners causes some excitement. *Genes Dev. 9:1811*.
79. Tontonoz, P., S. Singer, B. M. Forman, P. Sarraf, J. S. Fletcher, C. D. Fletcher, R. P. Brun, E. Mueller, S. Altiok, H. Oppenheim, et al. 1997. Terminal differentiation of human liposarcoma cells induced by ligands for peroxisome proliferators-activated receptor γ and the retinoid X receptor. *Proc. Nat. Acad. Sci. USA 94:237*.